R·I·T

Rochester Institute of Technology
Chester F. Carlson Center for Imaging Science
Digital Imaging and Remote Sensing Laboratory

Annual Report for the Academic Year 2008-2009

of the

Frederick & Anna B. Wiedman Professor

on the

Activities of the Digital Imaging and Remote Sensing Laboratory

Prepared by the DIRS Laboratory

Submitted by Professor John Schott

John R. Schott, Ph.D.
Frederick & Anna B. Wiedman Professor
Digital Imaging and Remote Sensing Laboratory
Chester F. Carlson Center for Imaging Science
Rochester Institute of Technology
54 Lomb Memorial Drive Rochester, NY 14623

Chester F. Carlson CENTER for IMAGING SCIENCE

Contents

List of Figures

1 Introduction

As you will see in the following pages, this has been another successful year for the DIRS Lab. This report briefly describes our research activities and publications. It is intended to highlight these activities but can not begin to delve into the details. We encourage you to contact the research team to discuss the details of any project further.

The lab continues to grow slowly and you will note some new faces in the Personnel section. Most significantly you'll note that Dr. David Messinger, who was acting head of the Lab during my sabbatical in 2007/2008 is now the permanent head of the Lab. Dave did an excellent job while I was away working on a book and we all decided that after nearly 30 years of managing paperwork and worrying staffing issues etc. it was time for me to focus on my own research interests and students. So the successes reported throughout this year's report are attributed to nearly two years with Dave at the helm. I hope those of you who don't yet know him, will remedy that through a visit to the Lab. I am sure you will continue to see the results of his sound management of the group over the coming years.

These annual reports have always reflected the joint activities of the Lab and the Wiedman Professor. To that end, let me briefly report on my activities as the Frederick and Anna B. Wiedman Professor. This Chair was funded by Frederick Wiedman to honor his parents and their commitment to educators. In addition to the research activities reported throughout the report, I'm also happy to report that the Polarimetric Remote Sensing book I worked on last year has been published and will be the foundation for a special topics course this fall. The book has already served as the basis for two short courses (one for industry and one for the government). The Wiedman endowment has also help fund three major initiatives supporting students. These are projects in new research areas where we are trying to build capabilities to enable us to establish longer term funded programs. These initiatives included the ongoing AANEE program to develop an improved analyst environment, and end-to-end polarimetric modeling and analysis project and evaluation of enhanced photon mapping tools in our DIRSIG modeling environment. These projects are all described in more detail in this report. Technically, they share a common theme of supporting students and providing the important seed funding to allow us to explore with our students directions we might never have an opportunity to develop with conventional funding sources.

I want to once again express my thanks to the late Mr. Wiedman for his generosity and to our extensive range of sponsors for your continued support of our research and academic programs.

John R. Schott, Ph.D.
Frederick and Anna B. Wiedman Professor
Digital Imaging and Remote Sensing Laboratory
Chester F. Carlson Center for Imaging Science
Rochester Institute of Technology

2 DIRS Laboratory Overview

The Digital Imaging and Remote Sensing (DIRS) Laboratory is a research group within the Chester F. Carlson Center for Imaging Science. Our work focuses on the development of hardware and software tools to facilitate the extraction of information from remotely sensed data of the earth and the education of students who will continue this work for government agencies and private industry.

The DIRS group is made up of faculty and research staff working with over 30 students ranging from the Baccalaureate through Doctoral level. Most students are degree candidates in Imaging Science, but students from other departments, such as Engineering, Physics, and Mathematics are often part of the student population supporting our research initiatives. This year also saw the inclusion of several high school interns who were provided the opportunity to participate in research projects and learn more about imaging science.

2.1 Laboratory Organization

The DIRS laboratory is managed using a matrix approach where faculty and senior staff manage programs to generate research results, student theses, and meet sponsor requirements. The research staff, organized into three overlapping groups managed by leaders, supports the needs of the research programs.

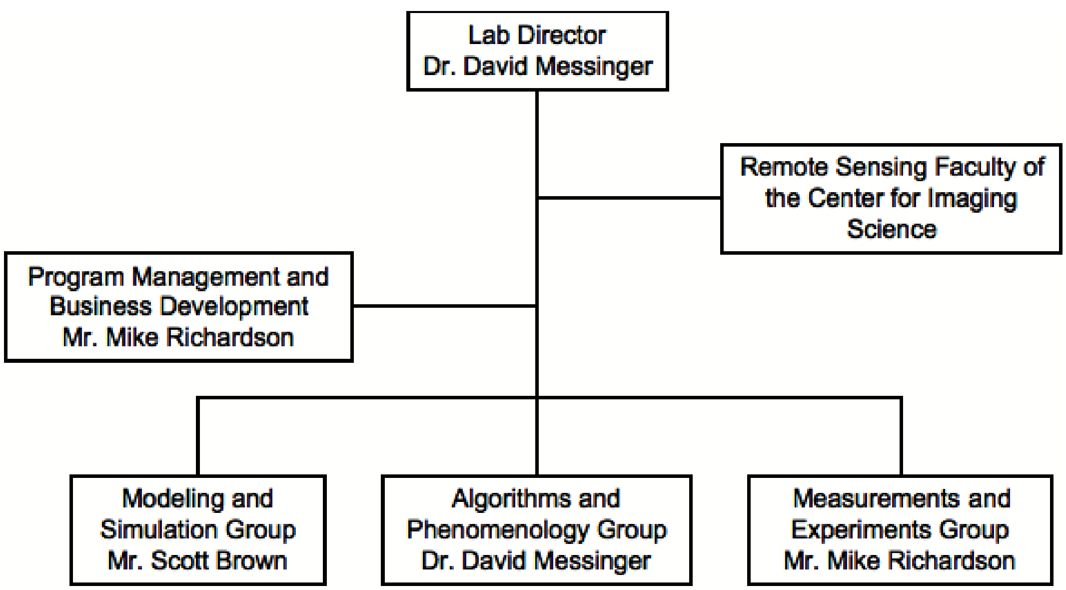

Figure 2.1-1: DIRS laboratory organization

The Laboratory of Imaging Algorithms and Systems (LIAS) is a parallel laboratory with the Center for Imaging Science which also conducts remote sensing research typically with a more user-oriented engineering scope. DIRS and LIAS have several joint endeavors. The DIRS component of these activities is included below.

2.2 Laboratory Personnel

2.2.1 Faculty

The DIRS Laboratory counts 6 faculty members as affiliated with the remote sensing research program. Of particular importance, Dr. John Kerekes was awarded tenure in the spring of 2009 to become effective at the beginning of the 2009-10 academic year. Additionally, Dr. Jan van Aardt joined the CIS faculty in the fall of 2008 to head the LIAS laboratory (mentioned above). Dr. van Aardt works primarily in environmental remote sensing and contributes to the overall remote sensing program at RIT greatly.

This year, Dr. John Schott was honored by the Education Committee of RIT's Board of Trustees as a recipient of the 2009 Trustee Scholarship Award. This award, established in 2005, is the premier RIT recognition for faculty contributions to scholarship, research and creative work.

Figure 2.2-2: Dr. John Schott, shown here with several of his current Ph.D. students, received the 2009 RIT Trustees Scholarship Award.

As taken from the official RIT announcement:

> *Schott has broad research and development experience in advanced technology for solving problems related to imaging science and remote sensing. He has served as the principal investigator on numerous research programs for both governmental and private sectors, including serving as a principal investigator for NASA's Landsat 7 Science Team. Schott also serves as a member of the Intelligence Science Board, which advises the intelligence community and the Director of National Intelligence.*
>
> *Schott's research has led to more than 100 technical publications, including a recent reference book on remote sensing, as well as co-inventor status on two patents. In addition, he has been awarded more than $10 million in sponsored grants and projects over the last decade.*

Dr. John Schott, Frederick and Anna B. Wiedman Professor
Research Interests: Hyperspectral data analysis and algorithm development; multi and hyperspectral in-

strument development; synthetic scene simulation and modeling
Contact Information: schott@cis.rit.edu; 585-475-5508

Dr. Tony Vodacek, Associate Professor
Research Interests: Environmental applications of remote sensing; forest fire detection and monitoring; active and passive sensing of water quality
Contact Information: vodacek@cis.rit.edu; 585-475-7816

Dr. Carl Salvaggio, Associate Professor
Research Interests: Novel techniques and devices for optical property measurement; applied image processing and algorithm development; image simulation and modeling
Contact Information: salvaggio@cis.rit.edu; 585-475-6380

Dr. John Kerekes, Associate Professor
Research Interests: Image processing and algorithm development; image chain modeling and parametric analysis
Contact Information: kerekes@cis.rit.edu; 585-475-6996

Dr. David Messinger, Assistant Research Professor, DIRS Laboratory Director
Research Interests: Multi- and hyperspectral algorithm development; advanced mathematical approaches to spectral image processing
Contact Information: messinger@cis.rit.edu; 585-475-4538

Dr. Emmett Ientilucci, Assistant Research Professor,
Research Interests: Multi- and hyperspectral algorithm development; physics-based signature detection in hyperspectral imagery; low-light level imaging systems
Contact Information: ientilucci@cis.rit.edu; 585-475-7778

Figure 2.2-3: DIRS faculty and staff members members.

2.2.2 Organization by Group

The research staff in the DIRS lab continues to be loosely aligned into groups based on focus area. This past year we added three research staff: Dr. Brent Bartlett joined the group in the fall as a postdoctoral research fellow while Chad Forrest and Caitlin Hart joined the group in the spring of 2009.

Modeling and Simulation Group:
Mr. Scott Brown, Group Lead: `brown@cis.rit.edu`; 585-298-9505
Mr. Niek Sanders: `sanders@cis.rit.edu`
Dr. Michael Gartley: `gartley@cis.rit.edu`; 585-475-7194
Dr. Adam Goodenough: `goodenough@cis.rit.edu`
Mr. David Pogorzala: `pogorzala@cis.rit.edu`; 585-475-5388

Algorithms and Phenomenology Group:
Dr. David Messinger, Group Lead: `messinger@cis.rit.edu`; 585-475-4538
Dr. Emmett Ientilucci: `ientilucci@cis.rit.edu`; 585-475-7778
Dr. Rolando Raqueño: `rolando@cis.rit.edu`; 585-475-6907
Mr. Chad Forrest: `forrest@cis.rit.edu`; 585-475-6686
Ms. Caitlin Hart: `hart@cis.rit.edu`; 585-475-4388

Measurements and Experiments Group:
Mr. Michael Richardson, Group Lead: `richardson@cis.rit.edu`; 585-475-5294
Ms. Nina Raqueño: `nina@cis.rit.edu`; 585-475-7676
Dr. Brent Bartlett: `bartlett@cis.rit.edu`; 585-475-5037

Administrative Support:
Ms. Cindy Schultz: `schultz@cis.rit.edu`; 585-475-5508

2.2.3 Student Researchers

Two of the DIRS researchers were honored in the fall of 2008 with scholarships from the US Geospatial Intelligence Foundation (USGIF) for their work in Remote Sensing as applied to Geospatial Analysis. These awards were competed across the nation. Phil Salvaggio was awarded the undergraduate student award, and Jamie Albano was awarded the graduate student award.

Below are listed the students pursuing research in the DIRS laboratory as of June 30, 2009:

Traditional students:
BS (9)

Juliet Bernstein	Ally Flickner	David Kelbe
Christina Kucerak	Katie Salvaggio	Phil Salvaggio
Erin Schmidtmann	Eugenie Song	Amanda Ziemann

MS (10)

Kelly Canham	Colin Doody	Tim Doster
Kenny Fourspring	Matt Heimbueger	Justin Kwong
Joseph McGlintchy	David Nilosek	Danielle Simmons
Michael Zelinski		

Ph.D. (15)

Jamie Albano	May Arsenovic	Bin Chen	Jacob Clements
Chabitha Devaraj	Aaron Gerace	Shea Hagstrom	Lingfei Meng
Ryan Mercovich	Matt Montanaro	Nima Pahlevan	Sarah Paul
Ariel Schlamm	Jacqueline Speir	Alvin Spivey	

Candian Forces and US Air Force officers enrolled in the MS and Ph.D. programs as of June 30, 2009 (10):

Diane Sarrazin (MS)	Cliff Anderson (Ph.D.)	Brian Flusche (Ph.D.)	Shawn Higbee (Ph.D.)
Alfredo Lugo (MS)	Jonathan Miller (MS)	Michael Pressnar (Ph.D.)	Tony Rizutto (MS)
Karl Walli (Ph.D.)	Aaron Wiener (Ph.D.)		

Figure 2.2-4: DIRS participation in the IEEE International Geoscience and Remote Sensing Symposium in summer 2008.

2.3 Theses Defended in Past Year

- Josef Bishoff, MS, "Target Detection Using Oblique Hyperspectral Imagery; a Domain Trade Study"
- Frank Padula, MS, "Historic Thermal Calibration of the Landsat 5 TM Through an Improved Physics Based Approach"
- Matt Turk, MS, "A homography-based multiple-camera person-tracking algorithm"

- Marcus Stefanou, Ph.D., “Spectral image utility for target detection applications”
- Scott Klempner, Ph.D., “Statistical modeling of radiometric error propagation in support of hyperspectral imaging inversion and optimized ground sensor network design”
- Brian Daniel, Ph.D., “A System Study of Sparse Aperture Sensors in Remote Sensing Applications with Explicit Phase Retrieval”
- Matthew Montanaro, Ph.D., “Thermal Radiometric Modeling of Mechanical Draft Cooling Towers”

Figure 2.3-5: Dr. Schott with a Corona Recovery Capsule at the Smithsonian Air & Space Museum (Mike Richardson in the background).

3 Research Project Summaries

3.1 LandSat Reflective Band Calibration Using Pesudo-Invariant Sites

Sponsor: NASA

Principal Investigator(s): Dr. John Schott
Research Team: Cliff Anderson

Project Description:
The long term calibration history of the Landsat 5 (L5) TM instrument has recently been defined using a time history of desert sites in Northern Africa. This trend is based on the assumption that the atmosphere is invariant and the reflectance of each site is approximately constant and Lambertian over time. As a result, the top of the atmosphere reflection is assumed constant when corrected for variations in the solar illumination angle and earth-sun distance. While this is true to first order and provides the current best estimate and the basis for all current temporal calibration, there are multiple known sources of residual error in the data. The two believed to be most significant and addressable are bidirectional reflectance (BRDF) and atmospheric variation from observation to observation. The major research thrust over the last year has been to develop a site BRDF both from satellite data and from a physics based model using DIRSIG.

The results of the satellite image derived BRDFs indicated the ability to correct some of the residual errors in the calibration data. Fig. 1 shows the calibration data for L5 Band 3 as blue triangles. The coefficients for the Torrance Sparrow BRDF model were found using a Levenberg-Marquardt regression. This model was then used to flatten out the original calibration data. The results are the red squares in Fig. 3.1-6. This shows approximately a 15% reduction in residual error.

While the BRDF models derived from satellite data showed some ability to correct for the site, evidence existed that the model assumptions were breaking down due to the extreme topography of sand dunes that make up the site. As a result, the next phase in this research is to model the site using DIRSIG. Each of the 75 available calibration days are being modeled using an ASTER derived digital elevation map. One of the initial modeled scenes is shown in Fig. 3.1-7.

Once all of the scenes are run, they will be processed in a similar manner as the actual L5 TM calibration data. The resulting database of simulated calibration values will be used to correct the original L5 TM calibration data for site BRDF effects.

Project Status:
This is an ongoing effort being conducted jointly with South Dakota State University which is responsible for the atmospheric correction component of the data. The goal is to produce a baseline compensation approach by Summer 2010.

3.2 LandSat Data Continuity Mission / Landsat Science Team

Sponsor: US Geological Survey

Principal Investigator(s): Dr. John Schott
Research Team: Aaron Gerace

Project Description:
The Landsat Data Continuity Missions (LDCM) Operational Land Imager (OLI) is a new sensor being developed by NASA for operation by the USGS. While Landsat instruments have traditionally been used for land-based studies, this five year effort evaluates LDCMs potential to be used for studying fresh and

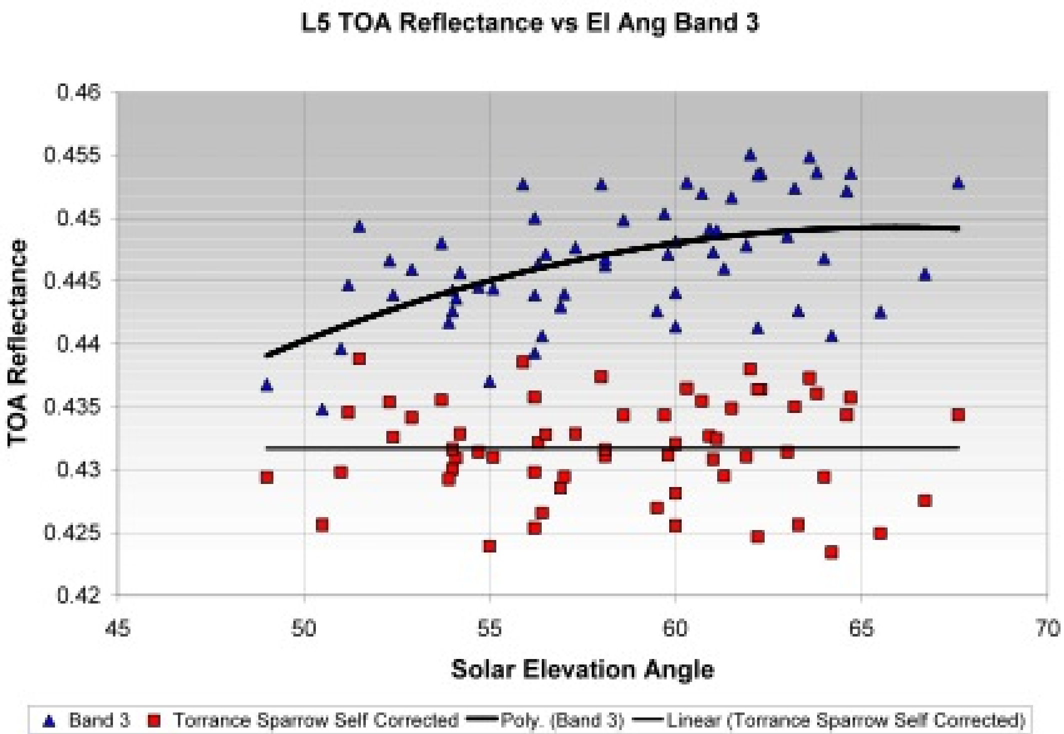

Figure 3.1-6: Landsat 5 Thematic Mapper Band 3 with Torrance Sparrow Self Correction

coastal waters. In the first phase of this research, the new features of LDCM were modeled and an experiment performed that tests its ability to retrieve the concentrations of three dominant coloring agents in coastal waters (i.e. chlorophyll (CHL), colored-dissolved organic material (CDOM) and suspended materials (SM)). Specifically, we are investigating how the addition of a deep-blue band, a 12-bit quantizer, and improved signal-to-noise ratios affect our ability to perform this constituent retrieval process. By using in-water radiative transfer models, the spectral reflectances of various water types can be predicted and converted to observed reflectances. The constituent retrieval process can then be performed for various sensors. The three sensors included in this study are the ETM+ sensor onboard Landsat 7 which reflects the current technology, LDCMs OLI instrument which represents the proposed technology, and an imaging spectrometer AVIRIS which represents the state-of-the-art technology. Each sensors ability to retrieve water constituents in the absence of atmospheric effects is shown in Table 3.2-1. Black values represent errors in retrieved concentrations while the red values (in parenthesis) express the errors as a percent of the range of observed concentrations (Errors of less than 15% are considered an acceptable goal).

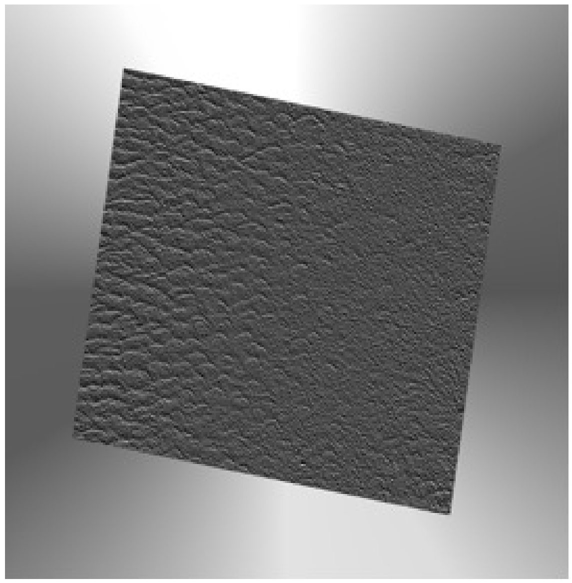

Figure 3.1-7: DIRSIG Rendering, Landsat 5 Thematic Mapper Band 2, 181/40 Correction Site

	CHL (μg/L)	SM (mg/L)	CDOM (1/m)
Spectral Coverage:			
AVIRIS	0.5 (0.7%)	0.1 (0.4%)	0.1 (0.7%)
ETM+	0.5 (0.7%)	0.6 (2.5%)	0.2 (1.4%)
LDCM	0.5 (0.7%)	0.5 (2.1%)	0.1 (0.7%)
Quantization:			
ETM+	5.7 (8.4%)	2.8 (11.7%)	1.7 (12.1%)
LDCM	1.2 (1.2%)	0.6 (2.5%)	0.2 (1.4%)
Noise & Quantization:			
ETM+	7.4 (10.9%)	4.8 (20.0%)	3.2 (22.9%)
LDCM	3.7 (5.4%)	1.2 (5.0%)	0.9 (6.4%)

Table 3.2-1: Average constituent retrieval errors introduced by each sensor. Red values express error as a percentage of the range of observed constituents in the scene.

The results are first shown for a noise free scenario, next with quantization noise included, and finally with instrument and quantization noise included. These results indicate that LDCMs OLI instrument exhibits the potential to be a useful tool for water resource studies. With its 30 meter resolution this could revolutionize the use of remote sensing for monitoring coastal and fresh water ecosystems.

In order to realize this potential, the second phase of this research evaluates our ability to perform the constituent retrieval process when atmospheric effects are included. An over-water atmospheric compensation algorithm has been developed that utilizes OLIs deep-blue band and near infrared band to effectively invert satellite observed radiances to surface reflectances. It is based on a phenomenon which can be observed in Figure 3.2-8. This figure shows the observed radiance spectra of a range of water samples that have been spectrally sampled to the OLI instrument. Notice how the data converge at the largest and shortest wavelengths. This indicates that if we observe a water body and the apparent reflectance is varying in these two extreme bands, the effect is dominated by atmospheric rather than in-water phenomena.

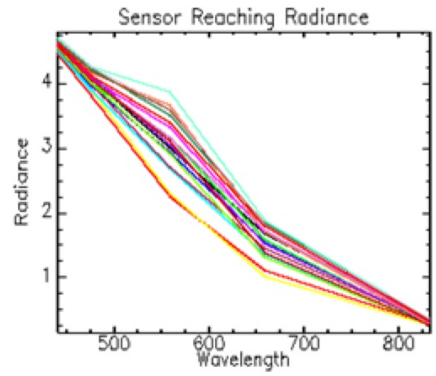

Figure 3.2-8: Plot of observed radiance for a range of water bodies with different constituents that have been spectrally sampled to Landsat OLI bands.

An experiment was conducted that tests our ability to perform constituent retrieval with the LDCM-specific over-water atmospheric compensation algorithm when atmospheric effects are included. As in the first phase of this research, an in-water radiative transfer model was used to obtain spectral reflectances of various water types. In this phase, however, atmospheric effects for a typical mid-latitude summer scene are simulated with the Moderate Resolution Transmittance Code (MODTRAN), which can be used to convert spectral reflectances to observed radiances. These sensor-reaching radiances are used in conjunction with the atmospheric compensation algorithm to perform the constituent retrieval process. The results of the retrieval process are shown in Table 3.2-2.

	CHL (μg/L)	SM (mg/L)	CDOM (1/m)	Avg. Chosen Visibility
Pixel-by-Pixel				
No Noise	11.7%	5.0%	4.8%	-
N/Q	16.0%	8.5%	7.3%	-
Global Removal				
No Noise	7.8%	3.6%	4.2%	22.56
No Noise	10.9%	5.0%	5.9%	22.57

Table 3.2-2: Average constituent retrieval errors introduced by the LDCM sensor and the atmospheric compensation algorithm (expressed as percentage of the range of observed constituents) for the no noise case and with noise and quantization included.

These results indicate that if the atmosphere is removed on a scene-wide or global basis, we can perform the constituent retrieval process with the LDCM sensor and expect to obtain errors of 11% or less for the three constituents (which is within our goal of 15%).

Ongoing efforts focus on determining the utility of the LDCM-specific atmospheric compensation algorithm when performed with real data. Additionally, we are evaluating the ability to use OLI data as a tool to calibrate a hydrodynamic model of the Genesee River plume (Figure 3.2-9) as part of an effort to use Landsat to study aquatic ecosystems.

Figure 3.2-9: Landsat true color image of the Genesee River plume.

Project Status:
This project is ongoing.

3.3 Physics-Based Target Detection in Hyperspectral Imagery

Sponsor: IC Postdoctoral Research Fellowship

Principal Investigator(s): Dr. John Schott
Research Team: Dr. Emmett Ientilucci

Project Description:
The overall goal of this effort is to develop improved physics-based modeling (PBM) approaches to target detection. More specifically, alternative methods for describing background / foreground spaces, improved physics-based computing infrastructure, visualization and incorporation of algorithms into a user friendly software environment.

Project Status 1: *BRDF and Physics Based Modeling*
Classical material detection involves the use of atmospheric compensation routines to provide estimates of ground leaving reflectance. It is here in this domain that measured target reflectance's are used in signature

matching schemes. Using an alternative physics based approach, one models the sensor reaching radiance given a target reflectance. Typically, the reflectance signature is one that is assumed to be Lambertian. However, many real man-made materials are not Lambertian. This paper addresses the ramifications of using a typical reflectance spectrum, assumed to be Lambertian, in an application such as target detection.

To test this assumption a DIRSIG scene was created with various painted (glossy) materials where others were oriented flat to the ground while some were tilted (see Figure 3.3-10. The BRDF's for these materials and geometry can be seen in Figure 3.3-11. Detection results in Figure 3.3-10(b) show that when looking for the green tipped panel, we not only get detections from the green non-tipped panel (as expected) but we get false alarms from the tan tipped panel because at this angle and BRDF, the spectra tend to converge. That is, the tan tipped panel starts to look like the green tipped panel.

(a)

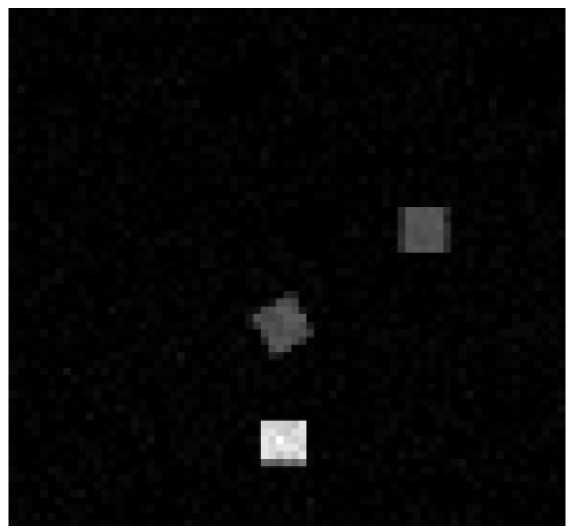

(b)

Figure 3.3-10: Original hyperspectral DIRSIG test scene shown in (a) with detection of green tilted panel in (b). Notice the false alarm detection of the tan tilted panel because of its similar BRDF to the green tilted panel (both glossy materials are tilted at the same angle).

Project Status 2: *Tracking of Vehicles in HSI using Compensation and PBM Techniques*

For this study, two recently acquired data sets were evaluated each collected at a different time. For each of the two collects, there exits a calibrated radiance and atmospherically compensated cube. Vehicles were placed in one collect and then moved to a random location in the second collect. Material identification was performed on both collections using radiance and reflectance imagery (*i.e.,* four data cubes). In addition, a couple common detection schemes found in literature were applied to all four cubes. The end goal in this study is two fold. The first is to apply both radiance domain and reflectance domain processing to multiple data sets with the idea of tracking a common material through out the imagery. Investigation is into whether there is one type of processing chain (reflectance imagery using a GLRT, for example) that is preferred over another.

Results on the blind-test data set can be seen in Figure 3.3-12. Desired scores are to be found in the upper right hand corner of the plot. In terms of domain preference, the radiance domain has some of the highest scores associated with the easiest target V1. However, if we simply evaluate the domain preference using each detector separately, we see that the radiance domain is preferred using the GLRT while there is no

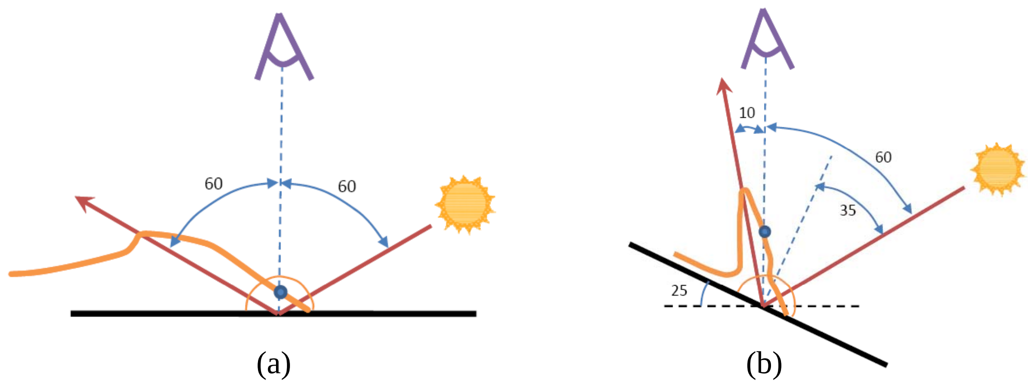

Figure 3.3-11: (a) View geometry and BRDF (for 550 nm light) for specular flat panel rotated zero degrees and (b) view geometry and BRDF (for 555 nm light) for tilted specular panel rotated 25 degrees.

preference when analyzing scores from the ACE algorithm alone.

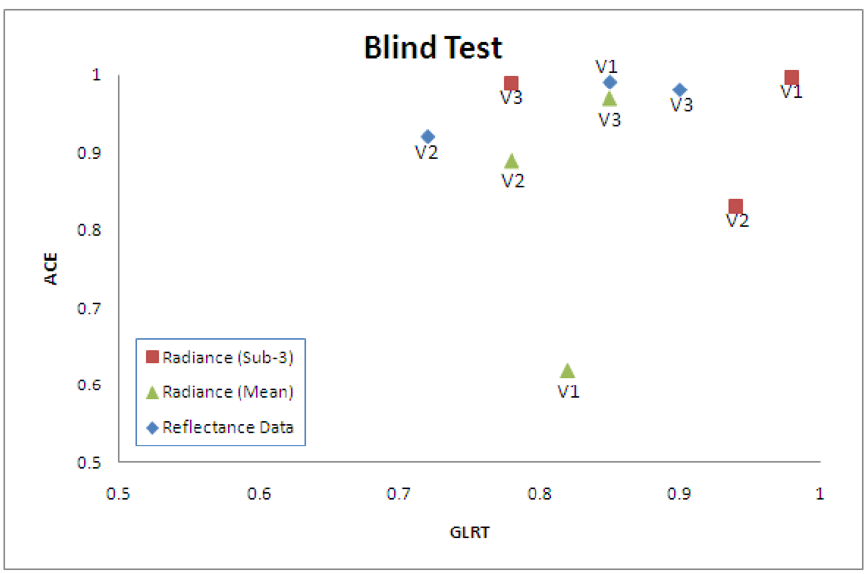

Figure 3.3-12: Plot comparing detection algorithm, domain, and target type for the blind-test imagery. The reflectance spectrum used was measured at the site, which was used in either reflectance processing or to build a target space for radiance domain processing.

3.4 Material Bi-Directional Reflectance Distribution Function Measurement

Sponsor: IC Postdoctoral Research Fellowship

Principal Investigator(s): Dr. Carl Salvaggio
Research Team: Dr. Brent Bartlett, Dr. Michael Gartley

Project Description:

In many remote sensing applications spectro-polarimetric imagery is acquired of denied targets. This reality requires the development of collection methodologies coupled with modeling algorithms to obtain the pBRDF of remotely sensed samples. This can be accomplished by using in-scene calibration materials with specific reflectance and geometric properties. A modular spectro-polarimetric imager that can characterize these materials in the laboratory as well as image them in the field is proposed. This instrument will serve as an ideal platform for testing and validating a radiometrically rigorous p-BRDF retrieval tool.

Project Status:

In a given remote sensing scene, there is a complex mixture of radiance sources that illuminate a given sample. In particular, the downwelling radiance field can be highly linearly polarized and impart polarimetric signatures on the scene. This can make retrieving the p-BRDF of a material diffcult. To address this issue, a polarimetric panel cluster has been designed to allow for the empirical calibration of spectro-polarimetric imaging systems. Using known diffuse reflectance values for materials present in the scene, both diffuse and specular portions of the p-BRDF can be retrieved for glossy materials within the same scene. The modeling environment of DIRSIG, in conjunction with MODTRAN-P, has been used to model the collected scene and provide for additional input values required for the p-BRDF retrieval process. This process has been demonstrated for glossy paint panels with real scene data as seen in Figure 3.4-13.

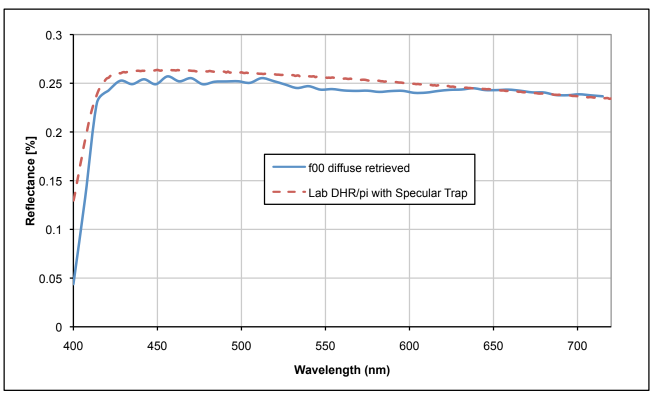

(a) Spectral diffuse BRDF compared with laboratory measurement.

Fresnel Theory Prediction

$$f_s(55°, 55°, 180°)\Omega_s = \begin{bmatrix} 0.081 & 0.081 & 0 \\ 0.081 & 0.081 & 0 \\ 0 & 0 & -0.005 \end{bmatrix}$$

Value derived from analysis of field imagery

$$f_s(55°, 55°, 180°)\Omega_s = \begin{bmatrix} 0.086 & 0.086 & 0 \\ 0.086 & 0.086 & 0 \\ 0 & 0 & -0.000 \end{bmatrix}$$

Retrieval Error

$$Percent\ Error = \begin{bmatrix} 0.5 & 0.5 & 0 \\ 0.5 & 0.5 & 0 \\ 0 & 0 & 0.5 \end{bmatrix}$$

(b) Specular p-BRDF results.

Figure 3.4-13: Results from retrieving the diffuse and specular p-BRDF from field data.

3.5 Microscale Surface and Contaminate Modeling for Radiometric Exploitation

Sponsor: IC Postdoctoral Research Fellowship

Principal Investigator(s): Dr. John Schott
Research Team: Dr. Michael Gartley

Project Description:

This project is aimed at developing, verifying, and applying a micro-scale surface reflectance model. The focus of the model is to predict the changes in surface optical properties in response to changes in surface condition and/or contamination with particulate and liquid contaminates. The resulting bi-directional reflectance and directional emissivity characterizations can be used in traditional, surface oriented radiometrycodes and signature-based algorithms. A modified version of DIRSIG (microDIRSIG) has been developed to perform these virtual spectral-polarimetricBRDF measurements of complex surface geometries.

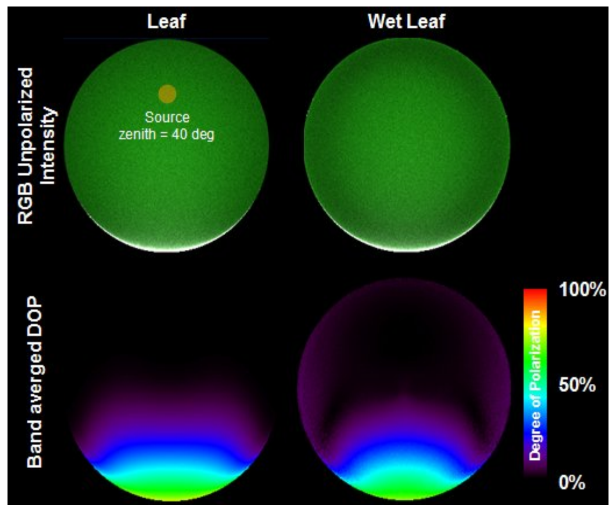

Figure 3.5-14: Example of microDIRSIG predictions of the spectral-polarimetric signature of a leaf in a dry (left) and wet (right) state.

Project Status:
The microDIRSIG model has been leveraged to create more realistic clutter environments for spectral-polarimetric image simulations conducted with the DIRSIG model. More specifically we have been able to create forests of trees that have leaves with various surface states (see Figure 3.5-14). Future work will examine the effect of the leaf surface state on detection probabilities for embedded man-made targets via ROC curve analysis.

Initial experimental measurements conducted to validate the modeling capability have shown good agreement (such as a soiled white paint) but more work remains to adequately link modeling inputs with geometry consistent with real surface contaminants. We have found both the microDIRSIG modeled and measured BRDF shapes for contaminated surfaces do not fit existing parameterized BRDF models well (such as the Beard-Maxwell model). Research is underway to examine a new functional form for a BRDF that adequetely captures all of the interesting phenomennology we have observed. In lew of developing such a parameterized BRDF model, we have created a hook within the DIRSIG software to ingest the raw spectral-polarimetric BRDF data (coming from either measurement or microDIRSIG simulations) and attribute scene elements for advanced simulations. Future research on this project will wrap up with adding an emissive modeling capability to predict emission signatures for various surface states.

3.6 Performance Driven Multi-modal Sensors

Sponsor: Air Force Office of Scientific Research (AFOSR)

Principal Investigator(s): Dr. John Kerekes, Dr. Zoran Ninkov, Dr. Alan Raisanen
Research Team: Michael Presnar, Lingfei Meng, Ken Fourspring; collaboration with Numerica, Inc. Dayton

Ohio

Project Description:
The objective of this project is to perform basic research in the development and use of integrated micro-electromechanical systems (MEMS) devices coupled with optics and solid state focal plane array technology for adaptive exploitation-driven multi-modality sensing suitable for ISR applications. In particular, we are investigating adaptive sensor designs that enable co-registered electro-optical imagery, video, polarization and spectral sensing in a robust compact unit. These designs are being explored together with research into real-time exploitation algorithms that can adaptively control the sensing modality and field-of-view to enable object tracking and monitoring specific to the situation. These device and algorithm research efforts are being conducted together with scene phenomenology modeling and simulation tools to perform comprehensive system-level performance analyses and demonstrations of the potential for the concepts to lead to transformational ISR capabilities.

Our approach for this effort is to explore feasible optical device constructs which through further research and development could lead to integrated imagery (both intensity and polarization), video and spectroscopic sensing together with the algorithms and scene phenomenology for adaptive sensing and tracking of objects of interest in a cluttered environment. This approach combines three interrelated research veins. 1) Sensor and Device Research. This research thrust is exploring conceptual designs and component modeling for integrated multi-modality optical sensors based on MEMS, digital micromirror, integrated Fabry-Perot, and high resolution lithography technologies. 2) Exploitation Driven Adaptive Sensing. This effort is working on the basic science of algorithms necessary to exploit, track and adaptively control the sensing parameters based on the scene phenomenology, observational geometry, and target information. 3) System Performance Modeling and Analysis. This third research vein provides the framework for end-to-end system modeling of the device concepts and processing algorithms and enables system level trade-off studies and performance predictions.

Project Status:
This year was the first year of the anticipated three-year project. The emphasis this year was on collecting data for model validation with the RIT Multi-object spectrometer (RITMOS) and developing a proof-of-principle model analysis. The RITMOS was operated in the laboratory and used to collect spectra of several test objects. These data were calibrated and prepared for use in validating the optical models. Models were developed for the RITMOS optical system using the FRED optical modeling software from Photon Engineering. Models of the TI Digital Micromirror Device (DMD) were developed in the multiphysics package COMSOL. DIRSIG simulations involving moving vehicles were generated and a first generation tracker developed using spectra as features to aid in the tracking. The emphasis of the second year will be on adding a polarization capability to the moving vehicle simulations, optical modeling and the tracking algorithms.

3.7 Accurate temperature retrieval of the exhausted air temperature from mechanical draft cooling towers for use with power plan process models

Sponsor: Department of Energy, Savannah River National Laboratory

Principal Investigator(s): Dr. Carl Salvaggio
Research Team: Dr. Matt Montanaro, Scott Brown, Dr. David Messinger, Dr. Alfred Garrett (SRNL)

Project Description:
Over the past three years, the Digital Imaging and Remote Sensing (DIRS) laboratory has been working toward a method of predicting the temperature estimation error that would be expected when deriving the exhausted air temperature from mechanical draft cooling towers (MDCT) using remote sensing approaches. The exhausted air temperature from these structures is a critical input to power plant process models developed the Savannah River National Laboratory (SRNL). DIRS is part of a team addressing the overall problem of power plant operating level prediction. Additional thermodynamics, hydrodynamics, and fluid flow engineers at SNRL are addressing other portions of this overall problem including the prediction of the air vectors and their temperature throughout these complex towers as well as the power plant operating level prediction based upon the observed drop in cooling water temperature across the condenser.

Since this target of interest is dynamic in time and appears within and against a complex radiometric background (Figure 3.7-15), radiometric derivation of temperature is very difficult to accomplish. This study has resulted in a method for producing a predictive model for the observed error in this measurement as a function of several operator-known scenario parameters. The DIRSIG and MODTRAN modeling environments have allowed for the creation of a multi-dimensional lookup table of error estimates as a function of the mechanical draft cooling tower's external temperature, the fan blade emissivity, the effective sky temperature, the sensor zenith angle, the ambient air temperature, the ambient dew point temperature, and the plume path length along the sensor-target path. These correction factor lookup tables were created and evaluated in several scenarios including fans on and fans off operation, fine and course spatial resolution imaging, as well as nadir and oblique viewing geometries.

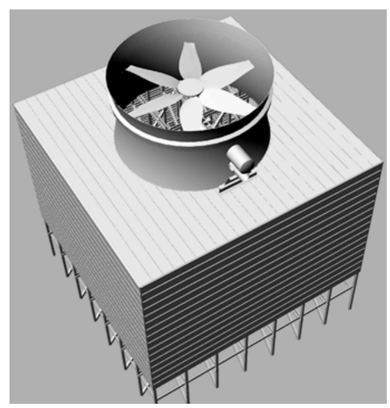

Figure 3.7-15: CAD drawing of a counter-flow MDCT used as input geometry for DIRSIG modeling.

Key findings during this year and through the conclusion of this project were that predicted errors from this approach fell within 1.3 K and 0.7 K of the actual temperature errors determined from ground truth measurements for nadir images for a mixed region of interest (including pixels from the tower cowling, fan blades, and all interior tower components) and a cavity region of interest (interior tower components only), respectively. Obliquely collected imagery performed worse due to fewer resolved pixels on target and increased path length through the water vapor plume (2.7 K and 1.7 K, respectively).

Project Status:
This project was completed in the Spring of 2009.

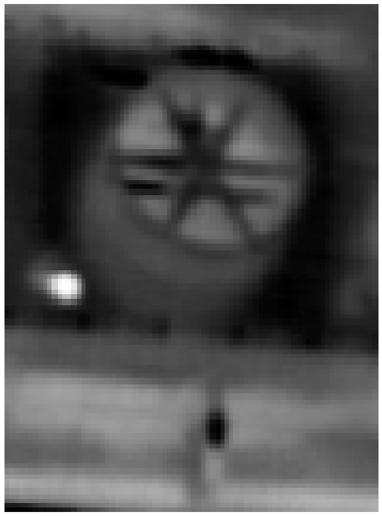

(a)

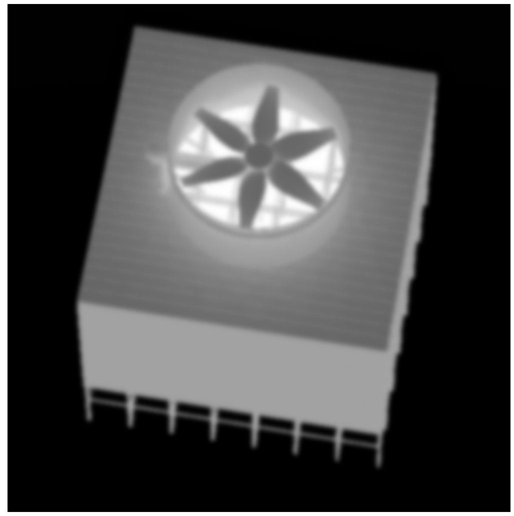

(b)

Figure 3.7-16: Actual longwave infrared image collected by the Savannah River National Laboratory at the Savannah River Site H-Area complex (a) along with a DIRSIG simulated version of a single cell of this tower (b).

3.8 Characterization of the influences of ice and snow on the radiometric field emanating from cooling lakes at cold site power plants

Sponsor: Department of Energy, Savannah River National Laboratory

Principal Investigator(s): Dr. Carl Salvaggio
Research Team: May Arsenovic, Jason Faulring, Dr. Brent Bartlett, Chad Forrest, Nina Raqueño, Michael Richardson, Donald McKeown, Dr. Alfred Garrett (SRNL)

Project Description:
The Department of Energy at their Savannah River National Laboratory (SRNL) has used remotely-sensed thermal infrared imagery for many years to evaluate the operating condition of power plants, specifically the determination of the plant operating level from the observed input and output cooling water temperature and their three-dimensional hydrodynamic code ALGE. This research effort is directed at assisting the SRNL scientists in extending this capability to perform in situations where the cooling lake is partially covered by ice in cold regions (Fig. 3.8-17). At these locations, the complete extent of the observable warm water discharge plume is not visible as it is partially obscured by the ice layer that forms at the surface. The ice not only obscures the plume, but based on its thickness, serves as an insulator that prevents heat loss from the lake therefore making the cooling system less efficient. The determination of the plant operating level is then based upon the determined temperature of the water in the melted region of the lake, the size of the melted area, and an estimate of the ice thickness across the frozen portions of the lake and the insulating effect that results.

During this past year, the combined DIRS and LIAS teams conducted winter data collection campaign. The campaign included eight (8) airborne collections (Figure 3.8-17) utilizing the RIT WASP sensing system that was modified to include in-flight blackbody calibration plates as well as hardened for cold weather operation. A ground collection program was deployed that included a rooftop camera system for monitoring the ice coverage on the lake surface (Figure 3.8-18), a shore-based weather station to measure

Figure 3.8-17: Longwave infrared image mosaic of the Midland Cogeneration Venture power plant in Midland, MI. This image was collected on January 26, 2009 at an altitude of 3,000 ft using the RIT WASP sensing system.

Figure 3.8-18: True color ground photograph collected with a Nikon D50 and a Sigma fisheye lens (left) of the MCV cooling pond from the plant roof. The geometric distortions were removed from this image producing the "defished" image on the right which was used to determine percent ice coverage on the lake.

air temperature, relative humidity, wind velocity, downwelling thermal and solar irradiance, and precipitation quantity (Figure 3.8-19), as well as five (5) buoys to measure the vertical temperature profile of the lake at one (1) foot increments and ice thickness (Figure 3.8-20). The image and ground-based data was remotely collected daily via a cellular data network and automatically posted to the Web at http://dirsapps.cis.rit.edu/doe/cold_site_power/. This site provides the investigators with access to all the data as well as a large number of visualization tools for analytical use.

There were many lessons learned during this first collection season that have led to two (2) subsequent buoy redesign processes to improve buoy stability, measure the orientation of the buoy relative to the water/ice surface, provide a calibrated surface temperature measurement using on-board hardware, as well as harden the design to survive the harsh winter conditions encountered.

Growing out of this project is a complementary study of surface temperature prediction of a water surface. A novel approach is being pursued to determine the skin temperature of the liquid surface based upon first-principles physics and engineering concepts. This approach is different from all the published models that have been in use for decades and hope to provide a better surface temperature estimate for improved sensor calibration performance.

Project Status:

Figure 3.8-19: Eppley pyranometer and pyrgeometer that make up part of the shore-based weather station used on this ground collection campaign. The frigid conditions are obvious from ice layer that formed on the instrumentation.

(a) (b)

Figure 3.8-20: Deployed buoys ganesha (a) and surya (b). Buoy stability was a problem during the first season due to the massive forces imparted on the devices by the shifting ice layer on the lake.

This project is ongoing and scheduled for completion in 2011.

3.9 Accurate Radiometric Temperature Measurements Using Thermal Infrared Imagery of Small Targets, Physics-Based Modeling, and Companion High-Resolution Optical Image Data Sets

Sponsor: Department of Energy

Principal Investigator(s): Dr. Carl Salvaggio
Research Team: Sarah Paul (Graduate Student), David Nilosek (Graduate Student), Chad Forrest, Scott Brown, Adam Goodenough, Michael Gartley

Project Description:
The US Department of Energy has an interest in accurately determining the temperature of a small object using aerial longwave infrared (LWIR) imagery. Accurate temperature extraction from a target, large or small, requires quality knowledge about the parameters that lead to the sensor-reaching radiance. In the LWIR portion of the electromagnetic spectrum, the optical properties of the target (most importantly the emissivity), the atmosphere and its effects on radiative transfer, and the sensor's calibration and spectral response characteristics are major contributing factors to the sensor-reaching radiance. Additionally, the point spread function (PSF) is a characteristic of all optical systems that spreads an incoming signal spatially across the detector. For large, uniform targets this spatial spreading is not a problem. The number of photons forced out of one path to a detector element end up in the path of any possible neighboring detector elements and on average, the correct number of photons end up back in the proper locations. However, for small targets (on the order of 4 ground sample distances or less), the photons being scattered away are "replaced" by photons from adjacent materials. Whereas in the previous case they were being replaced with photons at the same energy level. This mixing of photons at different energy levels from multiple target materials results in an inaccurate radiance value on a small number of or subpixel basis and therefore produce inaccurate temperature estimates. The question of how to account for the photons from the target that are scattered out of their original paths and for the photons from the adjacent material that have been scattered into the target path is one of the many questions that this project seeks to answer.

Current approaches to the small-target radiometry problem try to account for the scattered photons by way of a linear systems approach. This approach employs traditional frequency domain restoration techniques to take the energy from photons that were spread by the PSF and return them to the proper location. This method is not ideal for a number of reasons. The point spread function of the entire system includes the blurring due to platform motion as well as atmospheric scattering. These parameters are not typically included in the solution and as such the processes produce errant answers. Additionally, the frequency domain techniques have been shown to be effective for targets that occupy several pixels in a scene, not for small targets. This is due to the fact that a target occupying only a 4x4 pixels area essentially only has edge pixels that border an adjacent material, as stated previously, once the optical and system-level blurring have occurred.

To illustrate this a simulation in IDL was done where a target and a background were created with radiance values of 12 and 6 [W/m^2 sr μm], respectively. A system point spread function (assuming no atmosphere or platform motion) was applied to the image as well as a small amount of noise to create what is referred to the recorded radiance in Table 3.9. The recovered radiance was calculated by applying a Wiener-Helstrom filter to the image in the frequency domain. This simulation was done for multiple target sizes where the target and the sensor were perfectly in phase, meaning that the edge of the target did not cross a pixel boundary. A summary of the results is found in Table 3.9.

Table 3.9-3: The recorded radiance and the recovered radiance from a different sized targets

Target size (in pixels)	Recorded Radiance	Recovered Radiance
6x6	10.55	12.07
4x4	10.09	12.05
3x3	9.67	10.23
2x2	9.04	9.55
1x1	7.86	7.98

As the size of the target gets smaller the recovered radiance value becomes less accurate (and it follows that the extracted temperature will do the same). Once the size of the target becomes 3x3 pixels there is only one pixel that does not border another material and therefore it cannot overcome the effect the mixing in of adjacent materials has on the radiance value.

This project will incorporate geometric scene information gather from multiple-view, higher resolution, visible image data. Having co-collected imagery at a higher resolution will enable us to understand the geometric structure of the scene at the subpixel level. This geometry will enable us to use the DIRSIG environment to evaluate a series of varying scenarios that might lead to the observed radiance seen on this lower resolution thermal imagery. This forward-chaining physic model approach will hopefully lead to a more robust temperature restoration technique. In order to extract this high-resolution, three dimensional geometric data from the multi-view imagery, the techniques of structure form motion used in the computer vision community will serve as a baseline for a unique approach that we have termed AeroSynth for three-dimensional dense point cloud extraction.

The current process for extracting a geometric physical model from a set of images is comprised of two parts. The first part of this process follows the basic structure from motion technique as previously mentioned. This process derives a sparse physical model of a scene as well as the fundamental matrices that describe the geometrical position of each camera relative to a base camera. The second part of this process uses properties of the fundamental matrices relating each camera together to extract a denser physical model. Using known camera information, these physical models are projected onto the base image and transformed to the X,Y,Z coordinate system.

The first step in the structure from motion technique is to extract a set of features from each image that can be used for an initial guess at point matching. The Scale Invariant Feature Transform (SIFT) is used to extract these features. SIFT converts the image into scale space by doing convolutions with Gaussian kernels of varying size, then extracts features by taking the difference between successive convolved images. The gradient of an area around the feature is calculated at many different angles and the peak response is chosen as the feature angle. These features are then described by the orientation of the area around the feature relative to the feature's angle. These descriptions are invariant to scale and rotation so similar features can be matched across different images using these descriptions.

The SIFT matching process yields many matches, although many of these matches are incorrect. These incorrect matches are removed from the system using the methodology known as RANdom SAmple Consensus (RANSAC). This process uses a property of the fundamental matrix called the correspondence condition. This condition says that any two matching points must be related by the fundamental matrix. This condition is used as the model in the RANSAC process. RANSAC uses this model to statistically find the inlying matches, RANSAC also solves for the fundamental matrix during this process. Figure 3.9-21 shows the process of finding initial matches using SIFT and then the inlying matches found using RANSAC with the correspondence condition.

The next step is to use the known fundamental matrix to extract a denser correspondence. This is done by using a property of stereo geometry. This property states that for every point in one image there exists a corresponding line in another image if the images are of the same feature. This line is thought of as a projection of a line extending out of the first camera from that point. This reduces the point-to-point matching search to a single line. A normalized cross-correlation is used to match the point from the first image along the line in the second image to find a match. This is done for every point over a region-of-interest.

Once all these matched points are found, basic photogrammetry is used to solve for the three-dimensional object coordinates. It is assumed that an initial estimate of all camera parameters is already known. A sparse bundle adjustment is used with the initial estimates of object coordinates and camera parameters to obtain a better estimate of the object coordinates. These object coordinates are then projected onto the base camera using the collinearity equations. The image coordinates are then transformed into X,Y space so each object coordinate can be mapped to an X,Y value. With the Z value already known from the photogrammetry calculations, this puts the object coordinates into X,Y,Z space. Once the georegistered three-dimensional point cloud of object coordinates has been created, it is facetized using Delaunay triangulation. This facetized model is mapped with an image of the target. Figure 3.9-22 shows the creation of one target from

Figure 3.9-21: The top set of images shows matching between the two images using the SIFT matching process. The bottom set of images shows the matching after the outlying matches have been thrown out using the RANSAC process. (Images courtesy of Pictometry International Corporation).

three images and how the point cloud is facetized and georegistered to the image. These models can be placed automatically placed in GIS programs because they are georegistered. In the future these models will also contain physical properties like spectra and thermal properties so they can be placed in DIRSIG simulation to aid the radiometric correction process.

Project Status:
This project is ongoing and scheduled for completion in 2011.

3.10 Characterization of Target Detection Performance in Oblique Angle Hyperspectral Imagery

Sponsor: VirtualScopics / Naval Research Laboratory

Principal Investigator(s): Dr. David Messinger
Research Team: Dr. Emmett Ientilucci, David Pogorzala, Josef Bishoff

Project Description:
This project was in support of a sensor development study being conducted by the Naval Research Laboratory and was a collaboration with VirtualScopics, a Rochester-based company. The goal was to characterize target detection algorithm performance for a hyperspectral sensor with an extreme oblique viewing geometry. Two approaches were used. First, using DIRSIG simulation capabilities, simulated scenes of the appropriate view geometry were created with appropriate targets embedded. The goal was to understand the radiometric effects of the longer atmospheric path on target detection performance and determine if they could be mitigated by performing target detection in the radiance domain. Traditional target detection is performed in the reflectance domain after the atmospheric effects have been removed from the image. Given the highly oblique view geometry, removal of such effects is very challenging and so detection in the radiance domain is appealing. To this end, a Physics-Based Signature detection scheme was developed that modeled the long and variable atmospheric path and its impacts on the target signature. Additionally, an in-scene method for atmospheric compensation was developed to test against the best possible scenario for atmospheric compensation. This study determined that while the challenges in target detection under these viewing circumstances are great, particularly in atmospheric conditions of low visibility, they can be overcome using the physics-based signature modeling approach. This approach outperformed the method

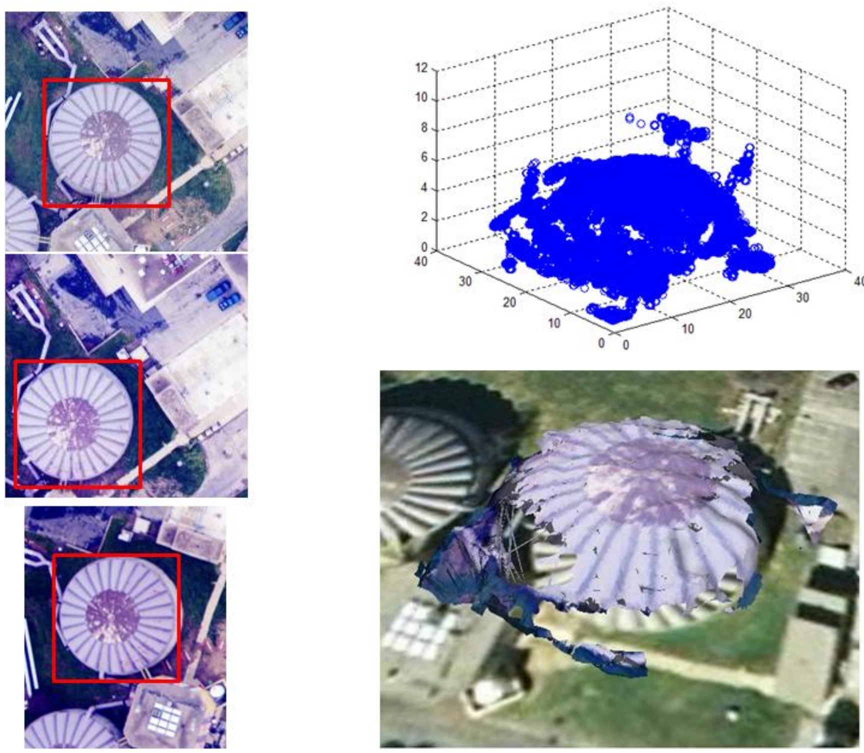

Figure 3.9-22: This shows the process of selecting a target in multiple images then using the images to create a dense point cloud of the target. Finally the dense point cloud is facetized, georegistered, and mapped with an image of the target.

of detection in the reflectance domain.

A second approach was to use the simulation capabilities of MODTRAN and FASSP to do a parametric analysis of detection performance as a function of pixel fill factor and other operational considerations. Figure 3.10-23 shows an example result from this study where the Probability of False Alarm was fixed, and the impacts on Probability of Detection were studied for variable pixel fill fraction and atmospheric visibility. Here, we see that for a given atmospheric visibility, a much larger pixel fill factor is required to achieve the same Probability of Detection under oblique viewing geometries than is required under a nadir viewing geometry. Results such as these impact operational considerations as well as sensor performance expectations.

Project Status:
This project was completed in the winter of 2008-2009.

3.11 Characterization of Physically Derived Signatures Spaces for Improved Spectral Unmixing

Sponsor: Naval Research Laboratory, National Geospatial-Intelligence Agency

Principal Investigator(s): Dr. Emmett Ientilucci

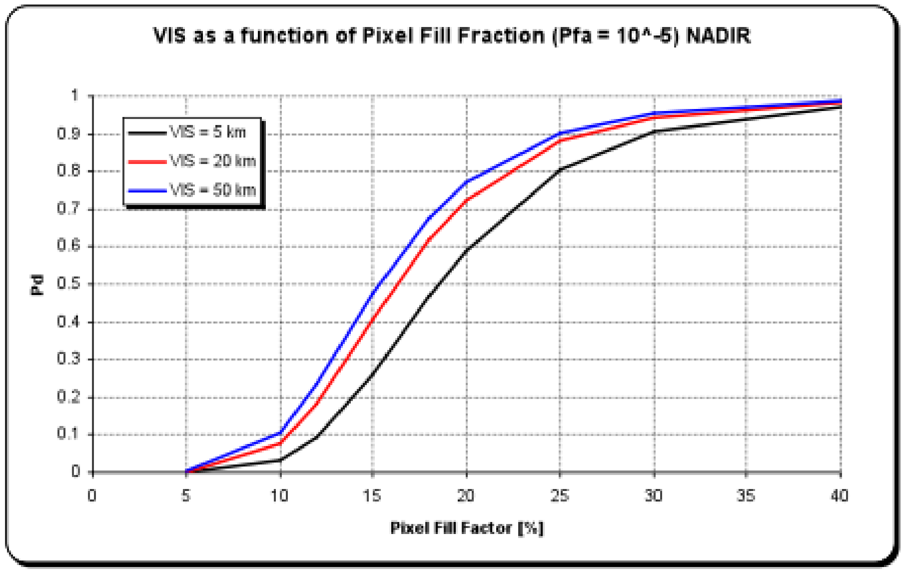

(a) Nadir view geometry

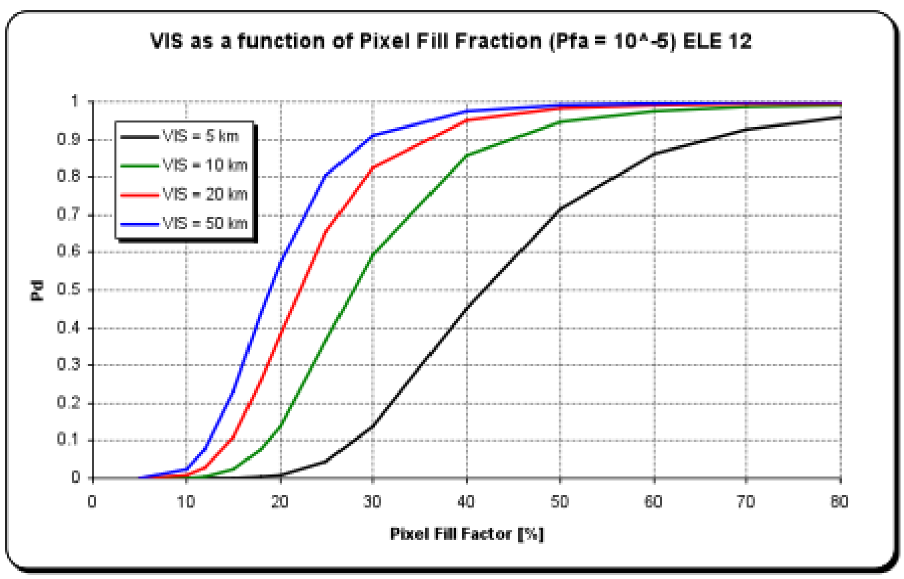

(b) Oblique view geometry

Figure 3.10-23: Visibility as a function of pixel fill fraction for a variety of atmospheric visibilities at a fixed probability of false alarm. (a) Nadir view geometry (b) Oblique view geometry (note the different scales in pixel fill factor).

Research Team: Dr. Emmett Ientilucci

Project Description:

This project supports an effort at NRL to develop a new generalized method for analyzing hyperspectral / multispectral data, based on the linear mixing approach. The work develops a generalized linear mixing model (GLMM) which incorporates an endmember grouping (EMG) technique as well as virtual endmembers generated through use of physics based modeling (PBM). In general, the concept of an endmember vector is generalized to an endmember subspace. This approach allows for modeling of the within-class variation of a material in a scene, while allowing for traditional mixture analysis, such as demixing/abundance estimation and fraction plane analysis, to proceed as usual. The method allows for virtual endmembers which are derived through use of physically derived signature spaces (PDSS). These virtual endmembers can produce an unmixing plane that is synonymous with typical target detection results. The project supplies NRL with signature spaces as well as user friendly tools (*i.e.*, ENVI plugins) that produce spaces based on a reduced set of MODTRAN runs.

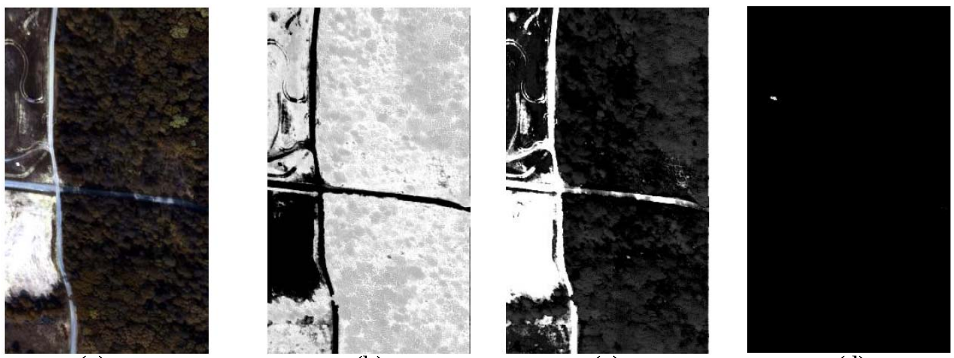

(a) (b) (c) (d)

Figure 3.11-24: Results of using the GLMM on HSI. (a) Original image, (b) grouped and demixed vegetation class, (c) grouped and demixed soil and asphalt class, (d) demixed target class using a virtual endmember subspace.

Project Status:
To date, ENVI plugin tools have been created that allow the user to create full (virtual) signature spaces with an overall reduction in the number of MODTRAN runs. Furthermore, these spaces, along with the GLMM, have been tested on real hyperspectral data (73 bands) with both unmixing and target detection in mind (see Figure 3.11-24). The results show a much tighter class map than can be produced by traditional linear unmixing approaches.

3.12 Characterization of Gaseous Plumes in the LWIR Using Bayesian Model Averaging

Sponsor: Pacific Northwest National Laboratory

Principal Investigator(s): Dr. David Messinger
Research Team: Shawn Higbee, Dr. Yolande Tra (RIT Math Department), Dr. Joe Voelkel (RIT Center for Quality and Applied Statistics)

Project Description:
The problem of gas plume detection and constituent identification is challenging for many reasons. Typically, once a plume has been detected in a thermal hyperspectral image, a linear regression, or a stepwise regression technique, is used to identify specific constituent gases in a plume. This method uses frequentist statistics. Here, a Bayesian approach was developed to utilize *a priori* information about the radiometry in the plume as well as spatial information in the plume to improve our ability to perform constituent identi-

fication particularly for very weak plumes. The project leverages pervious work in LWIR HSI temperature and emissivity separation to "take apart" a hyperspectral cube and then inject synthetic plumes into this real imagery. Figure 3.12-25 shows the spatial concentration template used to generate the plume (top) as well as the resulting radiance imagery (bottom) over a small portion of a larger hyperspectral image collected with the AHI sensor.

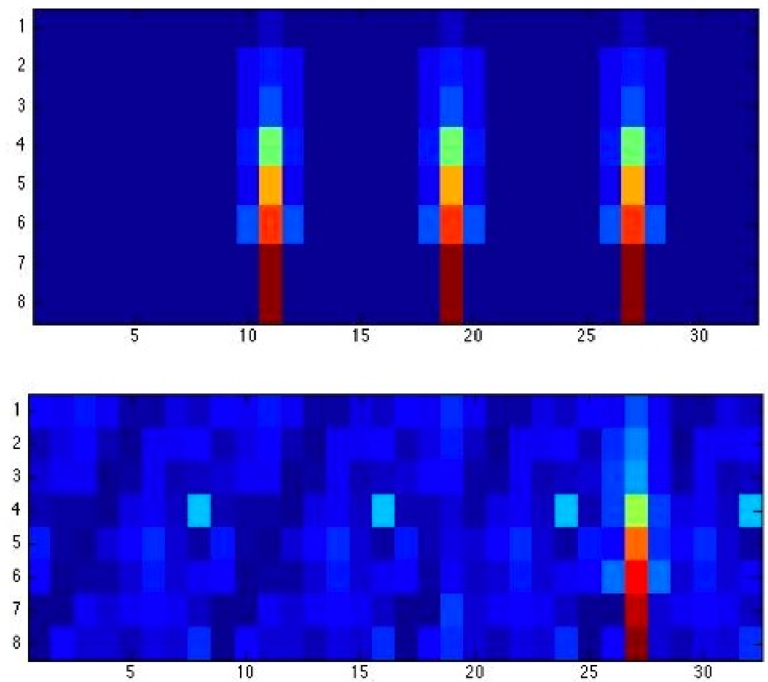

Figure 3.12-25: Spatial template (top) and resulting plume radiances for a variety of concentrations, here shown as four "tiled" images.

The use of a Bayesian framework to determine the best gas constituent model for each pixel requires estimation of complicated integral of prior and posterior probability functions. For this work, a Markov Chain Monte Carlo (MCMC) approach was used to numerically estimate these integrals. Sampling of the random variables was performed using Gibbs Variable Selection. One key finding was that degeneracy in the library of gas spectra used in the process dramatically impacts performance and a novel method was developed to "thin" the library using Variance Inflation Factors (VIF). The amount of thinning required depends on both the library contents and the sensor characteristics. VIF provides the user with a methodology to automatically thin the library for optimal performance.

In general, MCMC has been shown to outperform traditional frequentist approaches. Also, the use of *prior* information in the methodology provides a clear path for temporal and spatial aggregation methods to further improve confidence in the results.

Project Status:
This project will be completed in the summer of 2009.

3.13 Gitam Technologies SBIR Support

Sponsor: Air Force Research Laboratory Sensor's Directorate (AFRL/RY)

Principal Investigator(s): Dr. John Kerekes

Project Description:
Several research efforts are being conducted in partnership with Gitam Technologies, a small business located in Dayton, Ohio.

Project Status:
During 2008-09 RIT was a partner with Gitam on two Phase II Small Business Innovative Research (SBIR) grants. Both are planned for completion during the upcoming 2009-10 academic year.

3.13.1 Network Centric Urban Vigilance (SBIR Phase II)

Research Team: James Albano, Xiaofeng Fan, John Parkes, David Pogorzala

Project Description:
The primary goal of this effort has been to develop novel and effective HSI-based algorithms for multi-platform and cued fingerprinting, detection, recognition and tracking of dismounts, vehicles and other man-made objects in urban scenarios. In support of this goal, researchers at the Rochester Institute of Technology have contributed primarily through the generation of synthetic images using DIRSIG of a scene observed under varying illumination and observing conditions.

During this initial year of the two-year Phase II effort, hyperspectral imagery generated under Phase I was further analyzed and used to confirm the capability of using a radiance spectrum obtained under one condition as a target spectrum to find the target in a similar, but distinct, hyperspectral image. Various algorithms were also evaluated and the stochastic spectral matched filter was found to be more robust than the geometric adaptive subspace detector.

Project Status:
Reflectance spectra of vehicles, weapons, and human cadavers have been provided by Gitam and are now being cataloged and prepared for use in a high resolution DIRSIG simulation. These simulations will then be used to explore the multiplatform cuing and signature consistency across various environmental and sensor viewing situations. This project is planned for completion in May 2010.

3.13.2 Hyperspectral Detection of Chemical and Biological Agents Using Biosensors (SBIR Phase II)

Research Team: Danielle Simmons, Nina Raqueño, David Pogorzala

Project Description:
The goal of this project is to investigate the ability of hyperspectral imaging systems to detect subtle phenomenological changes in plants that have been genetically engineered to stop producing chlorophyll when exposed to trace amounts of hazardous chemicals or explosives. This research is in partnership with biologists at Colorado State University who are producing the genetically modified plants.

Sensor system design studies and scene simulations are being performed as part of engineering studies on the performance capabilities and design requirements to detect the subtle changes in the plant spectral reflectance with remote observing hyperspectral imaging sensors.

Project Status:

This project was initiated in late 2007 and will continue through late 2009. A spectral imagery data collection of the plants before, during, and after exposure to a TNT surrogate was made in August 2008. These data were further analyzed throughout 2008-09 and used to form the basis of synthetic imagery. While the plants showed minimal response due to a number of experimental factors, the data were helpful in exploring spectral band selection and in predicting detection performance. An additional collection is being planned for August 2009 during which the plants will be exposed to not only the hazardous chemical of interest, but also additional potential confusing sources such as stress or heavy fertilizer applications to study the potential for false benign detections.

3.14 Dynamic Analysis of Spectral Imagery

Sponsor: NGA University Research Initiative

Principal Investigator(s): Dr. David Messinger
Research Team: Ariel Schlamm, Timothy Doster (RIT Math Department), Dr. Bill Basener (RIT Math Department)

Project Description:
This project is a collaboration between DIRS and Dr. Bill Basener in the RIT Math department. The goal of the project is to develop advanced, non-linear, data-driven models of spectral imagery to improve exploitation, particularly in support of the problem of large area search. The project has funded graduate and undergraduate students from both the Center for Imaging Science and the Mathematics department at RIT. Under this project, methods have been developed to better estimate the inherent dimensionality of spectral imagery in an effort to determine the presence of man-made material in a subset (tile) of an image. This is done through a technique called Point Density Estimation. The Point Density Plot is developed for a set of spectral (see Figure 3.14-26) and can be interpreted to have three components: an "incline" and "transition", and a "tail". Each region of the plot measures a different aspect of the data distribution in the spectral space and can be used for exploitation. The incline measures the inherent dimensionality of the data near the center of the spectral cloud and has been shown to be indicative of the presence or absence of man-made materials in the pixel subset. The tail measures the outliers in the distribution and is being investigate for use in change detection and anomaly detection. The transition region is not yet fully understood.

The tail region has been shown to be particularly sensitive to non-natural changes in an image subset. Consequently, a methodology was developed to automatically estimate the length of the tail of the distribution for use a metric for changes in an image tile. Figure 3.14-27 shows the results of this change detection algorithm when applied to two hyperspectral images. In the first image (shown under the tiles) the vehicles are out in the open field; in the second they have been removed. The images are roughly registered and tiled. For each tile, the tail length is estimated and the change in tail length between the two images for each tile is calculated. The image shows the results of "turning on" tiles of the image as a function of the calculated delta tail length. Note that at higher thresholds the majority of the targets are still identified as being significant changes between the two images. This method of change detection is being further explored for application to multispectral imagery in addition to hyperspectral imagery.

Project Status:
This project was originally a two year effort scheduled to be complete in the fall of 2009. However, in the spring of 2008 the NGA awarded DIRS one of the option years in the contract to continue the research. This program will now be complete in the fall of 2010.

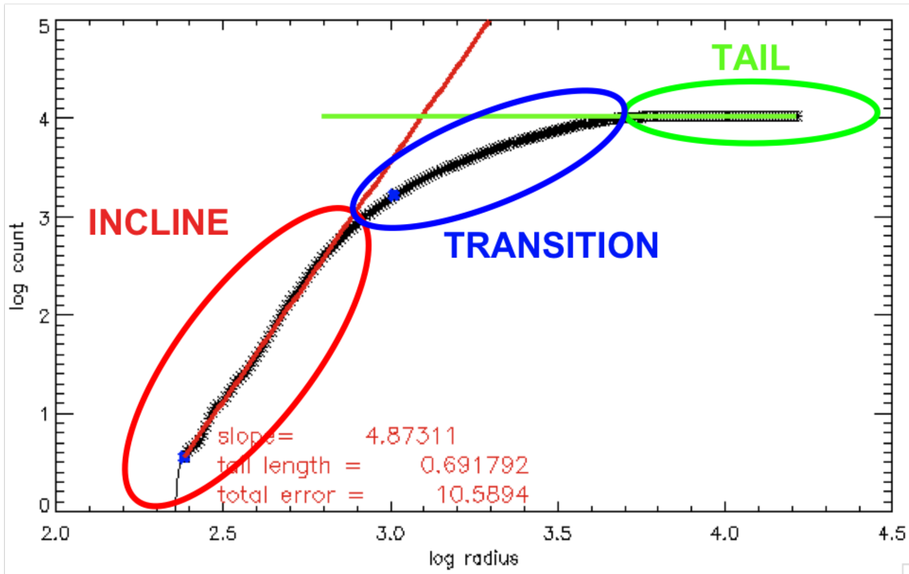

Figure 3.14-26: An example point density plot for a forested region from a hyperspectral image. The three-component model of the plot, "Incline", "Transition", and "Tail" regions are shown. Each region measures a different aspect of the data distribution in the spectral space and can be used for exploitation.

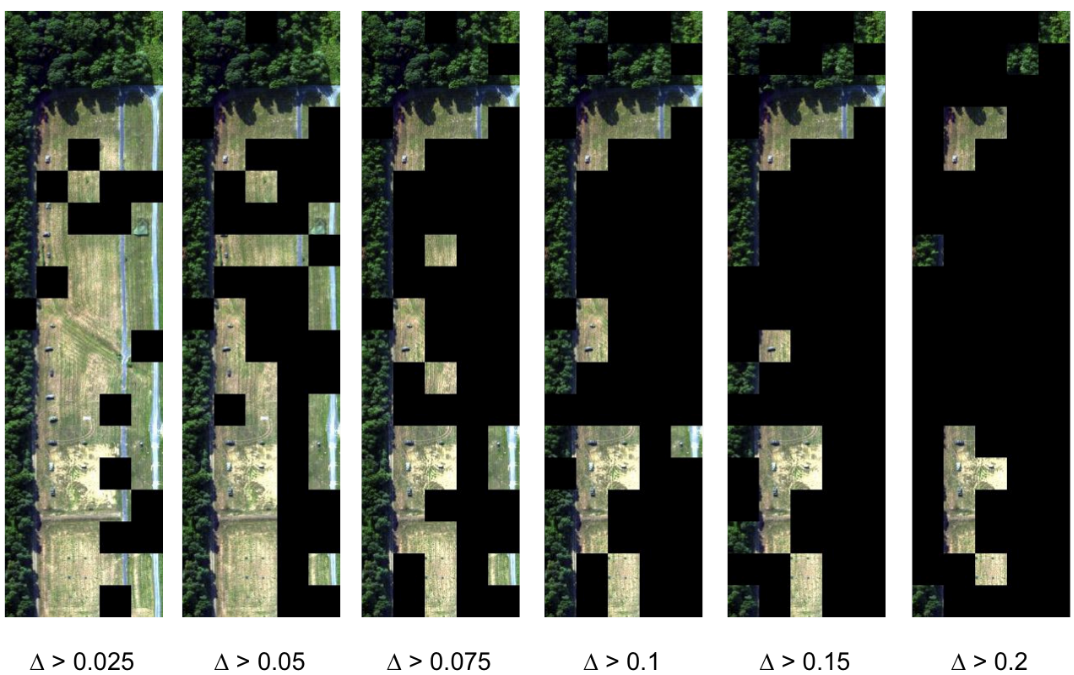

Figure 3.14-27: Results from the Point Density change detection algorithm as applied to hyperspectral data. Differences between the two images are the locations of the vehicles. Images show the identification of image tiles identified to have changed at various thresholds.

3.15 Remote Sensing for Archeological Studies of Oaxaca, Mexico

Sponsor: NASA

Principal Investigator(s): Dr. David Messinger, Dr. Bill Middleton (RIT College of Liberal Arts)
Research Team: Justin Kwong, Kelly Canham, Dr. John Kerekes, Dr. Tony Vodacek

Project Description:
In collaboration with archeologists at RIT and the University of Colorado, DIRS is supporting an ongoing study to understand the rise of the Zapotec culture in the Oaxaca Valley in southern Mexico. To date, over 25 images from the Hyperion sensor on board the EO-1 satellite have been collected. Hyperion is a hyperspectral imager with spectral coverage in the Visible / Near Infrared / Shortwave Infrared and spatial resolution of 30 m. The projects has two thrusts: one is to provide a large area coverage map showing detailed land use; the second is to perform further in-depth analysis on specific sites of interest. All imagery and results are being incorporated into the Google Earth visualization environment for ease of use by the archeologists while in the field. An example of the Google Earth implementation is shown in Figure 3.15-28. Here, the RGB composites for all of the flight lines collected are shown overlayed on the low

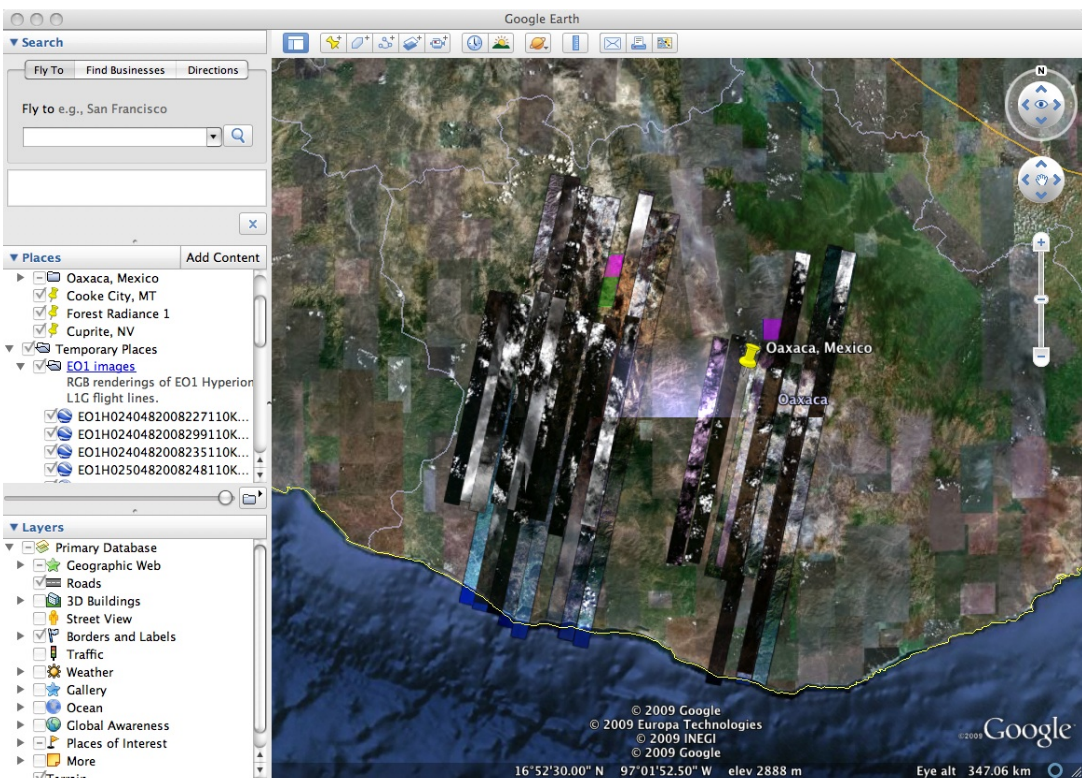

Figure 3.15-28: Google Earth interface for Hyperion data and derived products over Oaxaca, Mexico.

spatial resolution background image provided in Google Earth. Also shown (pink and green polygons in the background) are proposed high resolution collection areas to be acquired from commercially available, high spatial resolution sensors such as QuickBird (shown in Figure 3.15-29). These high resolution imagery will provide more detailed scene context for specific areas of interest.

Derived products from the hyperspectral imagery will eventually include large area land use maps as well

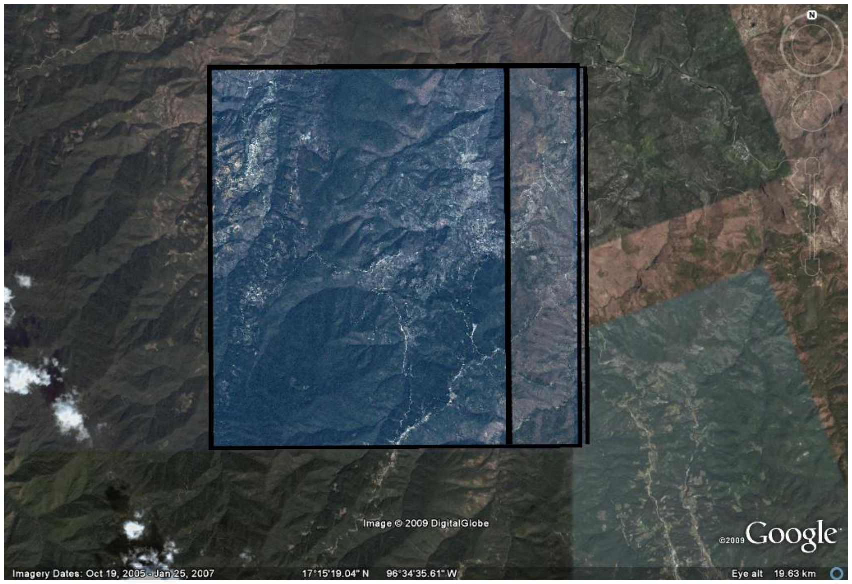

(a)

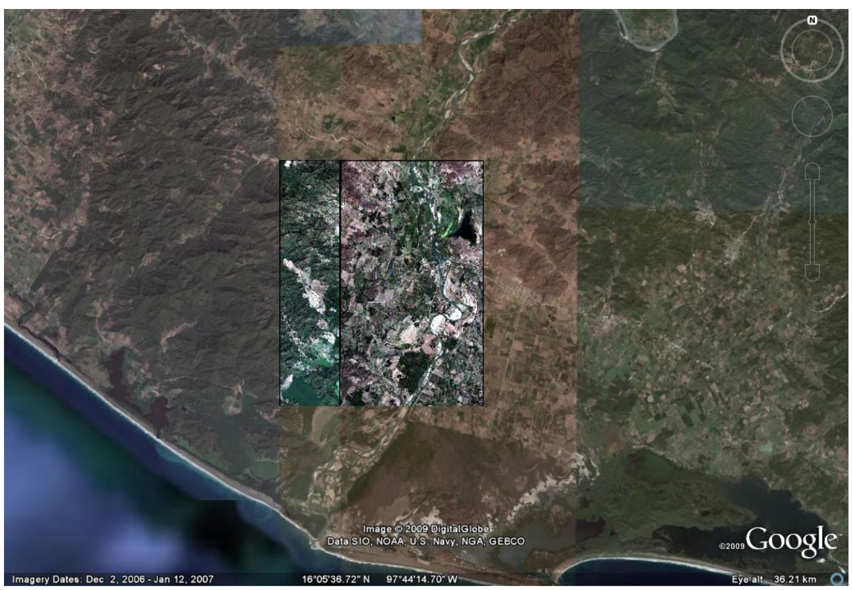

(b)

Figure 3.15-29: High resolution imagery from Digital Globe over (a) mountainous and (b) river regions in the Oaxaca, Mexico research site.

as the results of spectral unmixing. Additionally, specific geologic features (indicative of erosion, terracing, or river meander) of importance to the understanding of the evolution of the Zapotec culture will be identified using methods for anomaly and target detection. Ultimately, the data and results will be hosted in a web-based system for use by other archeologists studying this area.

Project Status:

This project is in the middle of a three year duration and will finish in 2011.

3.16 Modeling Support for the Common Sensor Payload

Sponsor: US Army Night Vision & Electronic Sensors Directorate (NVESD)

Principal Investigator(s): Scott Brown
Research Team: David Pogorzala, Niek Sanders

Project Description:
The US Army Common Sensor Payload (CSP) program tasked the Night Vision and Electronic Sensors Directorate (NVESD) to calibrate and modify existing sensor performance models to better support the CSP mission. These performance models predict the ability of soldiers to perform a specified military discrimination task using an EO/IR sensor system. The DIRS lab was subsequently tasked to develop a set of synthetic imagery for use in human perception testing. This imagery was to be used by NVESD to empirically measure the ability of persons to perform CSP-specific military discriminations. The imagery simulated a color visible sensor operating at 30 frames per second and represented a CSP on an appropriate aircraft and performing realistic mission scenarios.

Project Status:
The synthetic data set, created using the DIRSIG model, simulated a video sensor system mounted on an unmanned aerial vehicle (UAV) that loitered around an area of interest. Platform parameters such as altitude, aircraft speed and turning radius were modeled off a Predator B UAV. The motion of the aircraft was set to 115m/s at an altitude of 7,620m, and circling a target point at a radius of 4,400m. No platform jitter was added to the motion of the aircraft.

The base scene used for the simulation was MegaScene 1, a high-fidelity recreation of a region of northern Rochester, NY. MegaScene 1 depicts a largely residential, suburban-style neighborhood featuring a large number of houses and trees. Within the scene runs a major north-south thoroughfare, along which lies a large school complex. From this thoroughfare a number of residential side streets branch out and create a fairly complex road network.

Dynamic scene content was introduced to MegaScene 1 through the integration of the Simulation of Urban Mobility (SUMO) automotive traffic simulation tool with DIRSIG. The SUMO model is described by its development team as a "microscopic, space continuous and time discrete traffic simulation". This means that for every given discrete second during the simulation, each vehicle is tracked individually at a continuous (x, y) coordinate. For interfacing with DIRSIG, a microscopic model is preferred to a macroscopic one in which traffic is modeled as a bulk flow rate. Note that even though each vehicle is tracked individually, its calculated position and speed is a function of real-world traffic variables, including the state of vehicles in front of it, the number of lanes on the current road, and normal right-of-way traffic rules. The SUMO package also allows the user to explicitly define any number of routes, on which any number of vehicles can travel.

In order to integrate SUMO simulations with DIRSIG a road network of the MegaScene 1 area was created. Maps from Google Maps were imported into Inkscape, a vector-based graphics package, and assigned to a background layer. The network edges (lanes) and nodes (intersections) were then drawn atop the map and exported to SUMO in an XML format. Once the network had been generated, a series of routes were created for the vehicles to travel along. In an attempt to create a simulation that resembled real-world traffic flow a large number of routes, most of which traveled along the main thoroughfare for at least a portion of their journey, were generated. Once the network and the routes were defined in SUMO, the simulation was performed and the output was reformatted into a series DIRSIG inputs.

Once the vehicular traffic had been exported to DIRSIG the sensor was configured to the specifications laid out by NVESD. The detector consisted of a 1000x1000 array of 4 μm pixels, spaced at pixel pitch of 4 μm, and oversampled by a factor of three in both the x and y directions. Three bands were configured to match the spectral response of the CIE tristimulus curves (XYZ). The focal length was set at 108mm, resulting in a ground sample distance (GSD) of 0.33m. The dynamic platform motion, the dynamic scene content and the sensor were configured together, and 145 seconds of data were simulated at 30 frames per second. The rendering process was distributed across four dual-core and three quad-core systems, and took 63 total days to render. The output was 4440 individual frames of image data. A series of three of the rendered frames are shown in Figure 3.16-30.

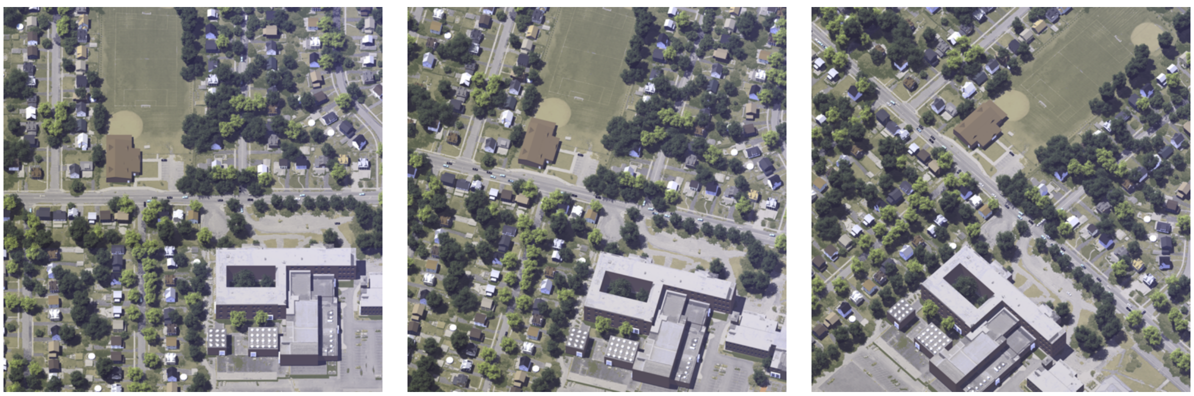

(a) (b) (c)

Figure 3.16-30: Three RGB frames from the CSP project. Each image has been autoscaled by its own image statistics. The orbiting motion of the aircraft can be inferred by the displacement of the static scene content as time increases from (a) t=0s, through (b) t=10s, and to (c) t=30s.

The raw images produced by DIRSIG were then processed and encoded into a number of video products. After a spatial blur was applied and the images were downsampled to 1000x1000 pixels, the radiance values were converted into digital counts through the application of a gain and bias. To illustrate the effect of this conversion on the final video product, two sets of gains and biases were applied. The first was a fixed gain and bias where values based on the image statistics of a single image were applied to each frame, while the second was an autoscale method in which each frame was scaled using its own statistics. Other variables that were exploited during the encoding process were the spatial extent (full frame, standard definition (SD) and high definition (HD)), the spectral output (RGB and panchromatic), and the system bandwidth (768 kbits/sec, 4 mbits/sec and 12 mbit/sec). Twenty-one final video products were encoded and delivered to NVESD.

3.17 Laboratory for Advanced Spectral Sensing Consortium (LASS)

3.17.1 SAR Simulation Research

Principal Investigator(s): Dr. Michael Gartley
Research Team: Dr. Adam Goodenough, Scott Brown

Project Description:
During 2008 we have initiated a focused effort that aims to integrate first principles radio frequency (RF) radiometry into the DIRSIG software model to support simulation of Synthetic Aperture Radar (SAR) collec-

tions. The scope of the project is to outfit DIRSIG with adequate RF optical properties, atmospheric models, antenna transmission and receive capabilities, and required post-processing tools that enable the user to simulate SAR collections over existing scene models (such as Megascene 1 and 2).

The new SAR capability is not merely an image processing trick, but truly simulates the transmission and reception of bundles of RF photons as they propogate between the antenna and scene elements. Leveraging the flexible platform motion and pointing capability of DIRSIG, the user can configure spotlight mode, stripmap mode, and even SAR-GMTI type collections (Figure 3.17-31). The raw outputs for SAR collections are the in phase "I" and quadrature signals "Q" digitized at the A/D converter level which may be optionally mixed with a reference signal to remove the carrier frequency. Post-processing tools, specific to the collection modality of interest, will be available in both compiled c++ programs and IDL engineering code to form simulated exploitation products. The added benefit to the community is a single simulation tool permitting analysis of remotely sensed phenomenology across multiple passive and active modalities and wavelength regions.

Project Status:
To date, the project has been a mix of straightforward model implementation and difficult research problems. Many of the RF atmospheric and optical property models are directly implemented from the published literature. The main challenge of the project has been to adapt a pure particle based software model (shooting and bouncing photon bundles and rays) to simulate wave based phenomenology such as interference and diffraction effects. Currently we are able to simulate antenna level diffraction patterns quite rigorously through simple Fourier analysis of antenna shapes. However integrating diffractive scattering behavior at the scene object level has been challenging and met with mixed levels of success. Additionally, maintaining coherency of the sampled scene points (for extended targets) has also posed an interesting challenge to us. We have developed multiple spatial sampling approaches that permit consistent sampling of the same scene points between pulses, even for moving objects. Future research will focus on improving the fidelity of our adaptation of the diffractive nature of RF optical scattering as well as improving code run time through improved sampling techniques.

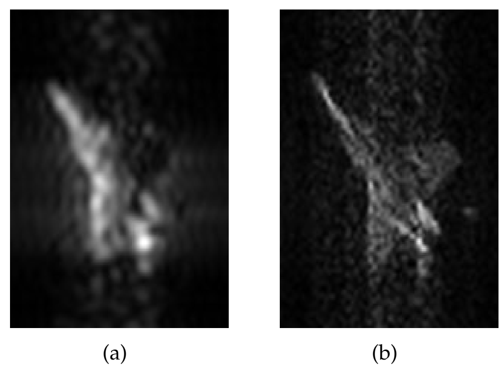

Figure 3.17-31: Examples of DIRSIG simulated SAR imagery collected in a stripmap (a) and spotlight (b) mode.

3.17.2 MegaScene 2 Status

Principal Investigator(s): Scott Brown
Research Team: David Pogorzala, Eugenie Song, Allison Flickner

Project Description:
The DIRSIG community benefits from the existence of large scale, detailed scenes. These MegaScenes are recreations of real world locations and are constructed with a high degree of both spatial and spectral fidelity, making them useful for a range of imaging tasks. The site for MegaScene 2 is Trona, CA, a small town located in the Mojave Desert. One of the attractive features of Trona is the large chemical processing facility that consist of numerous reserve tanks, pipes, buildings, and other industrial clutter. A byproduct of the plant is the unusual landscape nearby, consisting of waste discharge, evaporating ponds and mineral

deposits. These features, along with the complexity of the plant, the arid environment, and the mountainous landscape, all pose challenges to the modeling process. While preliminary versions of the scene are complete, the ultimate release will feature full-spectrum (0.4 - 14 μm) capability inside a 6km x 8km area at a pixel resolution of 0.5m.

Project Status:
A nominal first edition of MegaScene 2 was released in autumn of 2008. This version contained CAD models of all geometric entities (buildings, houses, etc.) attributed with, at a minimum, spectral reflectance data. All of the geometry was placed atop a facetized terrain model that was created using USGS DEM data. The (x, y) location of each model was matched to the objects real-world UTM (Zone 11) coordinate.

Notable features that the first release did not contain are robust terrain material maps and thermal capabilities. Extensive work has been done in the past year on finalizing a material map, with effort being focused in two fronts. One thrust has focused on smarter implementation of the material reflectance spectra collected by previous ground collection efforts. By redistributing the available measurements we were able to improve the visual texturing in the scene. Figure 3.17-32 depicts an RGB rendering of the scene both before and after the redistribution of material reflectance measurements.

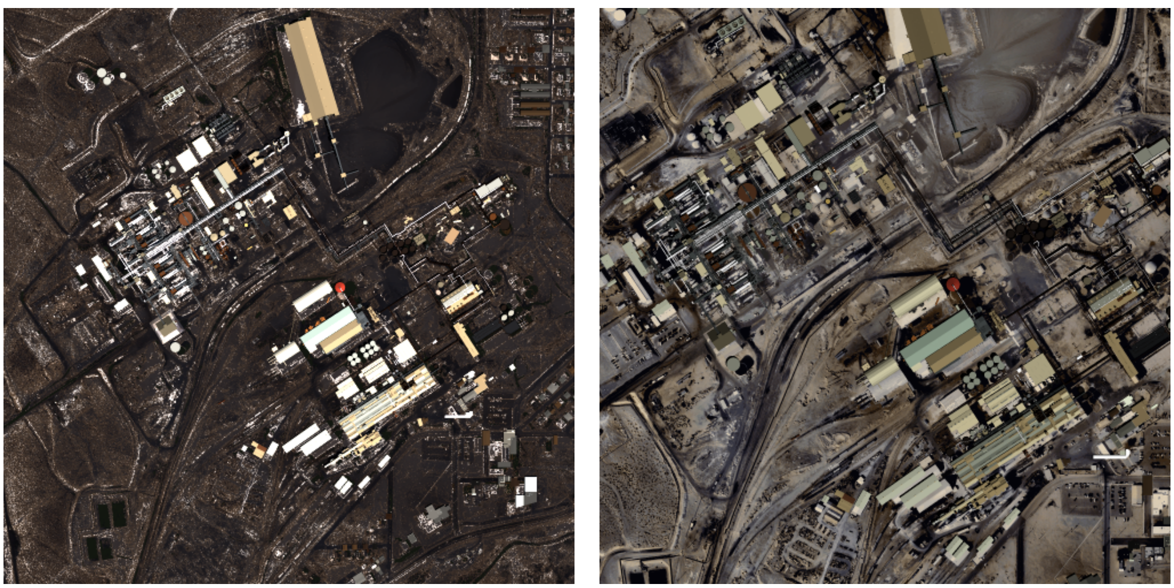

(a) (b)

Figure 3.17-32: RGB rendering of a portion of MegaScene 2 (a) before and (b) after improvements to the mapping of terrain materials.

The second focus in creating a new material map has been to utilize image data from the three infrared cameras of RITs WASP sensor. This sensor, which consists of a visible RGB, shortwave (SWIR), midwave (MWIR) and longwave (LWIR) camera, was used to map the MegaScene 2 area. Data from the RGB camera was processed and classified to create the first generation material map. Work is currently underway to process data from the three IR cameras in the hope that, when merged with the RGB imagery, a more robust material map can be made.

Another area of effort in the past year has been the addition of man-made light sources to the chemical plant, allowing a user to simulate low light level (*i.e.*, nighttime) imagery. In order to approximate a real industrial facility sources of various types were used in different locations. Streetlights that had been attributed with the spectral intensity distribution of a sodium vapor light were distributed throughout a parking lot and along a roadway. The doorways of several structures were illuminated from above by mercury vapor lamps. Fluorescent lights were also inserted in the interior of the office building. An example simulation of a nighttime image with the sources enabled is shown in Figure 3.17-33.

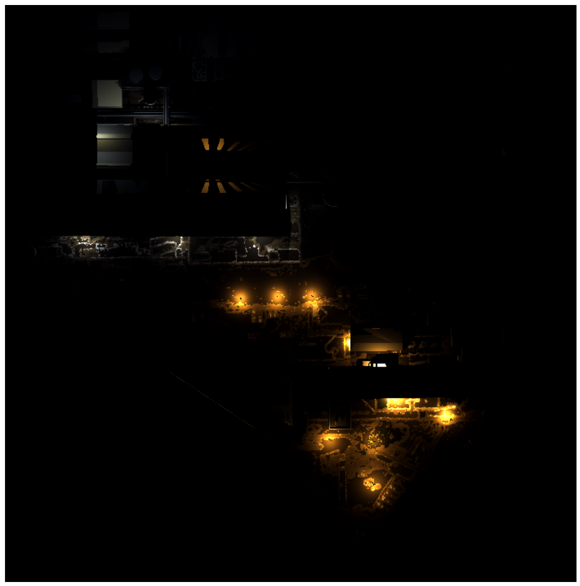

Figure 3.17-33: An RGB rendering of a nighttime image of the chemical facility in MegaScene 2. Secondary sources placed within the scene were enabled for this simulation.

3.17.3 Validation of DIRSIG Polarization Models

Principal Investigator(s): Dr. John Schott
Research Team: Chabitha Devaraj, Dr. Michael Gartley, Scott Brown

Project Description:
DIRSIG *validation of surface reflection polarization:*
The accuracy of surface reflection polarization predicted by DIRSIG is verified by analyzing the water surface reflected polarization pattern at sunrise/sunset. A unique polarization pattern occurs at low solar elevation resulting in an unnatural dark spot on water due to the reflected polarization of the vertically polarized sky near the horizon. The test scene within DIRSIG as shown in Figure 3.17-34(a), contains a hemispherical shaped object of water and a large flat plate below the geometry to represent a nonreflecting ground. This ensures that the polarization pattern of the water surface is determined predominantly by the surface reflected skylight. A hemisphere of water was used in the simulation so that the reflection of the entire sky dome can be observed on the water surface in a single image. A polarimetric image at 450 nm was rendered at 5 am on a clear day using a nadir looking framing array sensor. Figure 3.17-34(c) shows that the DIRSIG predicted reflection polarization matches with the theoretical reflection polarization pattern in Figure 3.17-34(b). This indicates the skylight polarization and surface reflection polarization of polarized radiance have been correctly integrated within the DIRSIG model.

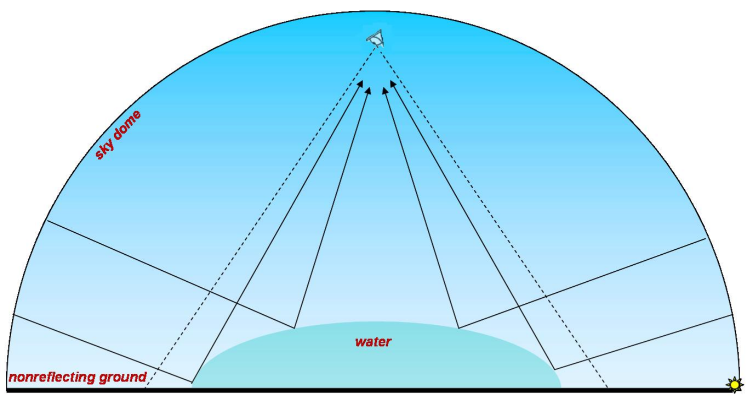

(a) DIRSIG simulation setup

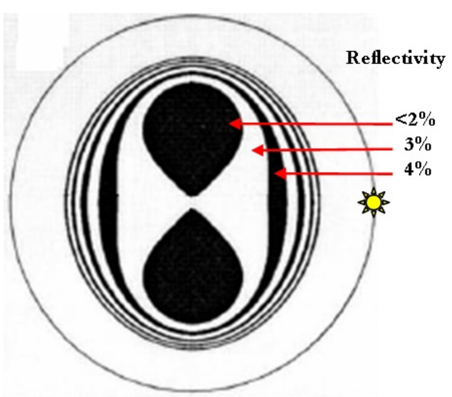

(b) Theoretical reflectivity pattern on flat water

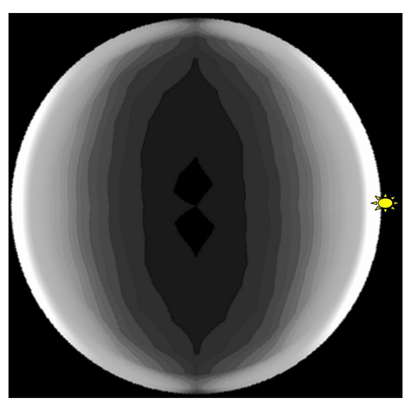

(c) DIRSIG water surface reflected skylight intensity pattern observed at sunrise

Figure 3.17-34: DIRSIG polarization validation of water reflectance

Material discriminability using polarimetric imagery:
To investigate the material discriminability in complex remote sensing scenes, a polarized version of the DIRSIG foxbat scene that contains different background materials such as grassland, soil, asphalt and urban materials like painted metals, concrete and aluminum was used. It can be seen from Figure 3.17-35(a) that the image was acquired at a low sun angle with a high sensor viewing angle in the backscattering direction. The inverse relationship between the intensity and DOP images can be confirmed by comparing the white and black aircraft in Figure 3.17-35(b).

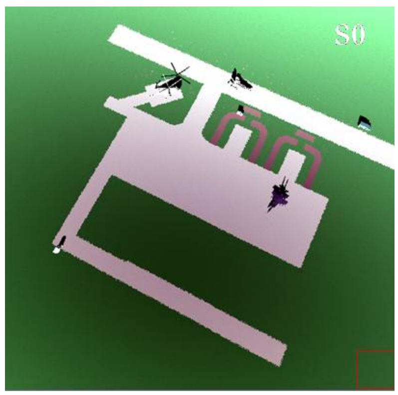

(a) Color composite of S0 intensity images

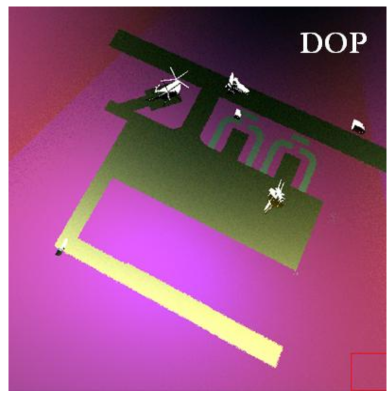

(b) Color composite of DOLP intensity images

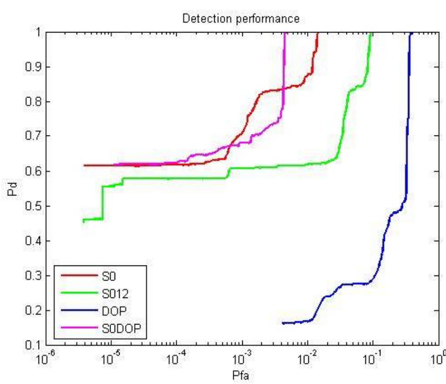

(c) ROC curve for RX detection performance

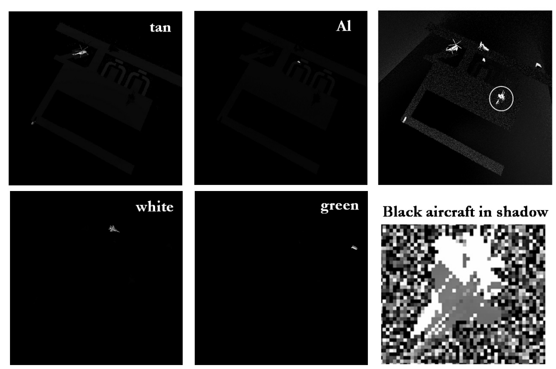

(d) OSP target fraction maps

Figure 3.17-35: DIRSIG polarization validation through detection algorithm performance.

The RX detection algorithm was applied on 4 different datasets and the ROC curves in Figure 3.17-35(c) show that the detection performance was improved when intensity images were combined with DOP images. Orthogonal Subspace Projection (OSP) based target classification was performed using S0 and S0DOP images and the resulting fraction maps are presented in Figure 3.17-35(d). It was identified that the black target aircraft cannot be detected using the intensity images. However, the polarization information was found to be useful in identifying such objects in shadow.

Project Status:
This project is ongoing and expected to be completed during the 2009 - 2010 academic year.

3.17.4 Persistent Surveillance at Night

Principal Investigator(s): Dr. John Schott
Research Team:Matthew Heimbueger

Project Description:
This project builds on earlier work that demonstrated that tracking of objects could be done more effectively if multiple spectral bands could be employed. In particular, it demonstrated that comparable performance could be achieved with multiband systems and slow frame rates or single band systems and high frame rates on multiband systems and large GSD or single bands systems and small GSD. However, these results were for daytime imaging conditions. Clearly persistent surveillance that only works in daylight is not persistent. Therefore, this study is aimed at determining if multiband sensing at night can improve the ability to track moving targets when compared to single band imaging. The approach uses a nighttime rooftop collection using a CCD camera, an image intensified camera and a longwave infrared camera. The analysis algorithms use the same approach used in the earlier daytime study.

Project Status:
This project is nearing completion and results are expected next year.

3.17.5 Multitemporal / Multispectral Image Exploitation

Principal Investigator(s): Dr. David Messinger
Research Team: Ryan Mercovich, Alfredo Lugo

Project Description:
Multitemporal / multispectral imagery is becoming more prevalent in the remote sensing field and this research project seeks to better understand the phenomenology associated to these problems and develop methods to exploit the imagery. There are two thrusts to this research, high spatial resolution multispectral imagery (pixels size $\approx$ 3m), and low resolution imagery (pixel size $\approx$ 30m). These two imaging modalities offer different challenges and opportunities for evaluation. While the low spatial resolution imagery, typical of the Landsat program, does not allow for analysis of small to moderate sized objects, it does allow for very large spatial coverage. The Landsat archive of imagery has recently been made openly available to the public and this research project seeks to understand how to best use the long temporal history of the archive for analysis purposes. The higher spatial resolution imagery is characteristic of the upcoming DigitalGlobe Worldview-2 sensor. This commercial satellite will provide imagery in eight spectral bands with a ground resolution of 3 m. Consequently, this allows for the analysis of smaller objects, but the background clutter will be far more complex. In both cases, the objective is to study targets, anomalies, and anomalous changes in the temporal nature of the data.

Figure 3.17-36 shows some preliminary results from processing high resolution data using a method taken from the literature and highlighting the clutter problem. The images were collected over the RIT campus using the RIT MISI hyperspectral sensor during the summer / fall of 2005 and spectrally resampled to the spectral resolution of the Worldview-2 sensor. The spatial ground resolution was approximately 3 m, providing approximately 1-2 pixels on objects such as cars. Clearly, there are differences between the two images, not only in the placements of the cars in the parking lots, but also in the health of the vegetation and the construction state of the collection pond. Figure 3.17-36(c) shows the result of applying the Hyperbolic Anomalous Change Detection tool to the two multispectral imagery. While several changes have been detected in the parking lots, most likely attributed to changes in the cars, there is also significant detected change in the forests where one would not have expected much change. This indicates the complexity of identifying and characterizing changes in high resolution imagery.

Project Status:

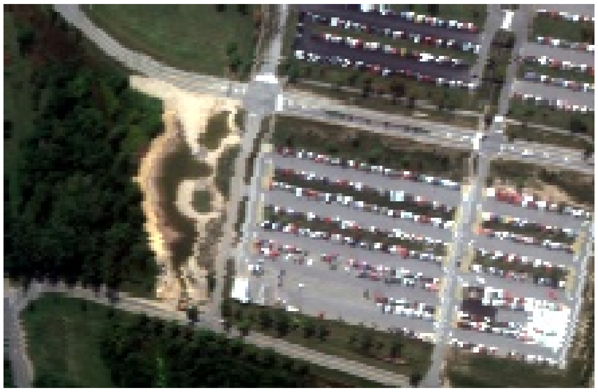

(a) Sep. 12, 2005

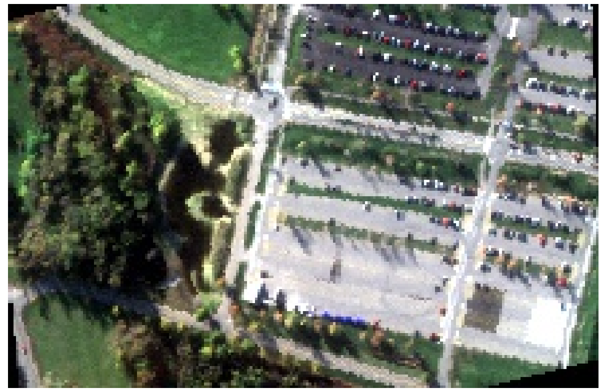

(b) Oct. 21, 2005

(c) Detected change

Figure 3.17-36: (a & b) Two images of the RIT campus collected with the MISI sensor, downsampled to the Worldview-2 spectral response. (c) The result of applying the Subpixel Hyperbolic Anomalous Change Detection tool to the two MS images.

This project was initiated in the Spring of 2009 and is ongoing.

3.17.6 Voxelized LIDAR Exploitation for Change Detection

Principal Investigator(s): Dr. David Messinger
Research Team:Shea Hagstrom

Project Description:
Sub-canopy scene reconstruction and change detection is a challenging problem due to the high level of occlusion. Two dimensional, traditional passive imagery can not easily differentiate between points above and below the canopy, but active, LIDAR imaging may provide a solution to this problem. Some pulses will penetrate the canopy due to gaps in the canopy, gaps due to leaf motion, and partial leaf transparency at the wavelength of the LIDAR. Here, we will be developing a voxelized methodology for analysis of the LIDAR data. Other methods for representation of the LIDAR point cloud include treating the data as raw points in three dimensional (x, y, z) space or constructing an approximate facetized surface geometry based on the 3-D points. The voxelized approach uses line of sigh information, in addition to the point

cloud data, to developed a *volume* representation of the data cloud. This approach promises benefits as it includes information about the entire path the LIDAR beam traversed as each return carries information about all of the voxels transversed along the path. However, the pulse source location and direction must be known and errors in this knowledge can lead to errors in the analysis results.

An approach is being developed that looks not only at the voxels in which the pulse is reflected, but also considers the transmission probabilities of the LIDAR beam along the path. This means that the voxels are non-isotropic (as transmission through the voxel has directional properties) and any derived properties are angle dependent. Consequently, collective data from multiple view points and times can be combined to form a more complete sub-canopy map of the scene. Also, more properties than simply “empty vs. full” can be derived from the return data and used for analysis.

Figure 3.17-37 shows a simple, early example of a test case of data. Figures 3.17-37(a) & 3.17-37(b) show simple RGB renderings of a tree on a flat plate (here colored blue for visualization purposes). Figures 3.17-37(c) & 3.17-37(d) show the simulated high resolution point cloud from a nadir-looking view geometry generated with 360,000 pulses. Using this simulated point cloud and the known collection geometry per pulse of the lidar, the probability of pulse transmission per voxel can estimated. Figure 3.17-38 shows this result for both overhead (a) and side (b) views. Note that the interior of the tree is darker indicating a lower probability that pulses will be transmitted into this portion of the canopy, while the outer region of the tree is lighter demonstrating a higher probability of pulse transmission. Note that the estimated transmission depends on the size of the voxels used in the analysis. Additional information that can be gained from this approach is a map of those voxels in which there is no information.

Project Status:
This research started in the Spring Quarter of 2009 and is ongoing. LIDAR data sets will be generated with DIRSIG for use in the algorithm development and testing stage. Multiple scenarios of a variety of complexity will be developed and the voxelized approach to sub-canopy scene reconstruction and change detection will be tested.

3.17.7 Segmented Aperture Space Telescope Image Quality and Image Utility Modeling

Principal Investigator(s): Dr. John Schott
Research Team: Michael Zelinski

Project Description:
The remote sensing community is constantly pushing technology forward to achieve better system performance, this is often done by improving signal to noise ratio, spatial resolution, and spectral resolution. However, improving one design parameter (such as spatial resolution) could detract from another (such as signal to noise). A flexible imaging system simulation tool capable of modeling the effects of changes in system parameters would be a great asset to design engineers. In words, this tool would manipulate a ”perfect” image and produce an output image identical to one physically created by the plausible design. Having such a tool available would make it possible to fully understand a design’s potential and understand the importance of changes in system parameters.

Modern space based remote sensing systems are taking on new forms using sparse and segmented apertures with lightweight mirrors. The reason for this is that the systems are constrained the by the size and weight tolerances of their launch vehicles and these types of telescopes can be folded into more compact payloads. The new designs come with new problems, many of which are related to the geometry and aberrations of the aperture. The system simulation tool developed in this effort is able to examine the effects of different amounts and types of aperture aberrations. Figure 3.17-39 demonstrates the model’s ability to produce segmented apertures that include piston, tip, tilt, and lightweight optic flimsy aberrations.

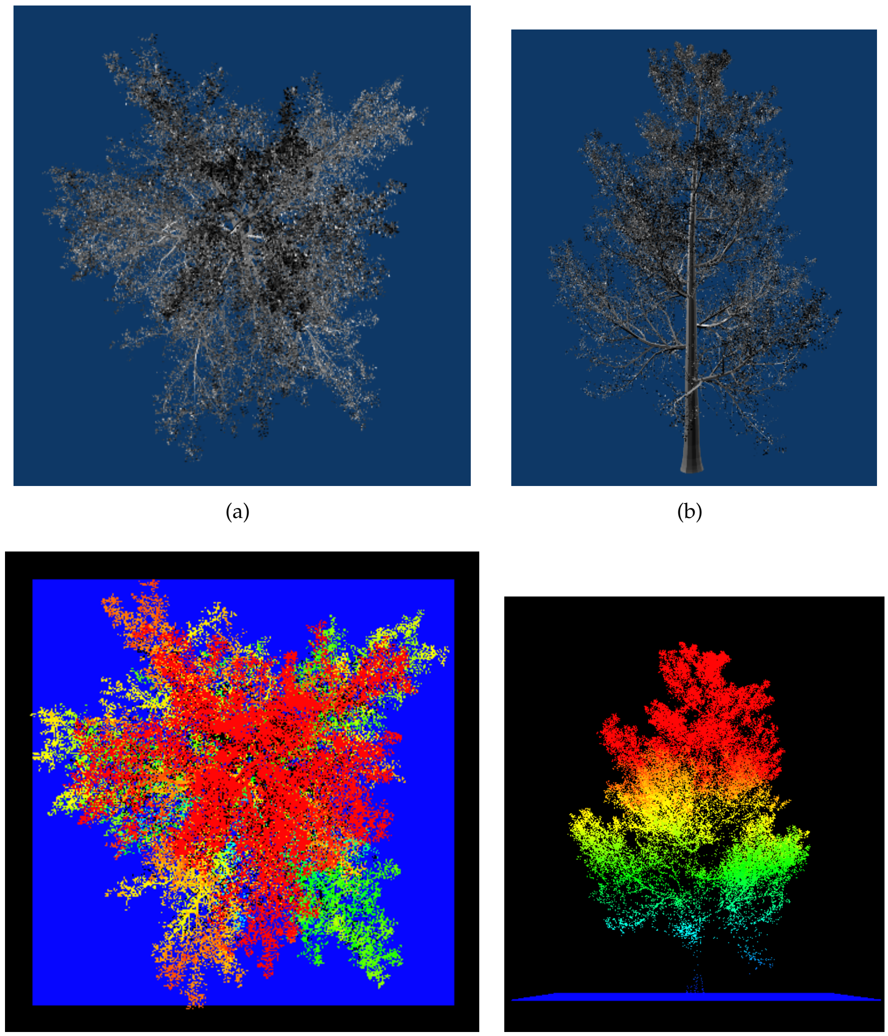

(a) (b) (c) (d)

Figure 3.17-37: Simple renderings of trees (a & b) and simulated point clouds (c & d) used to develop the methodology for sub-canopy detection using a voxelized methodology. (a) & (c) Overhead view. (b) & (d) Side view.

The imaging system simulation tool, based on linear systems and standard radiometry, is capable of accurately displaying the imagery created by plausible designs. Using this tool, several designs can be compared using image quality and image utility metrics. Image quality/utility is determined using three techniques. The first is an image quality prediction technique called the Generalized Image Quality Equation (GIQE) which relates system characteristics to the National Imagery Interpretability Rating Scale (NIIRS). Figure 3.17-40 shows results generated using the GIQE on the blue band for a 1m GSD system with a high SNR. However, because the aberrated sparse and segmented telescopes are not axially symmetric the GIQE cannot accurately predict image quality for these designs. The other two approaches are performance metrics tied to specific algorithms. These approaches don't actually define an image quality but allow systems to be ranked by their performance in a test of motion detection or a test of spatial target detection. A multispectral motion detection algorithm combined with motion truth show a given imaging system's ability to

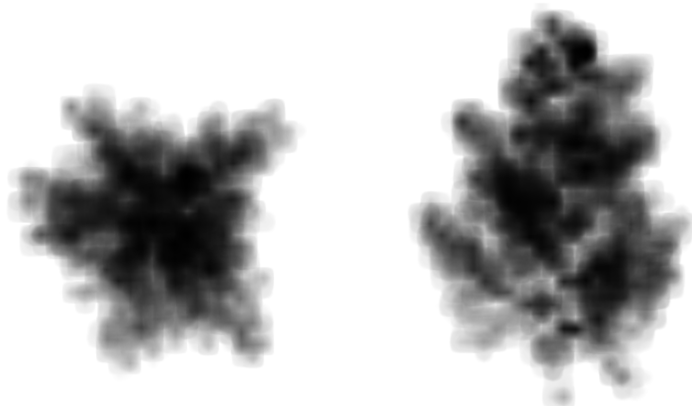

(a) (b)

Figure 3.17-38: Estimation of the tree transparency based on the voxelized approach to LIDAR point cloud analysis. (a) Overhead view. (b) Side view.

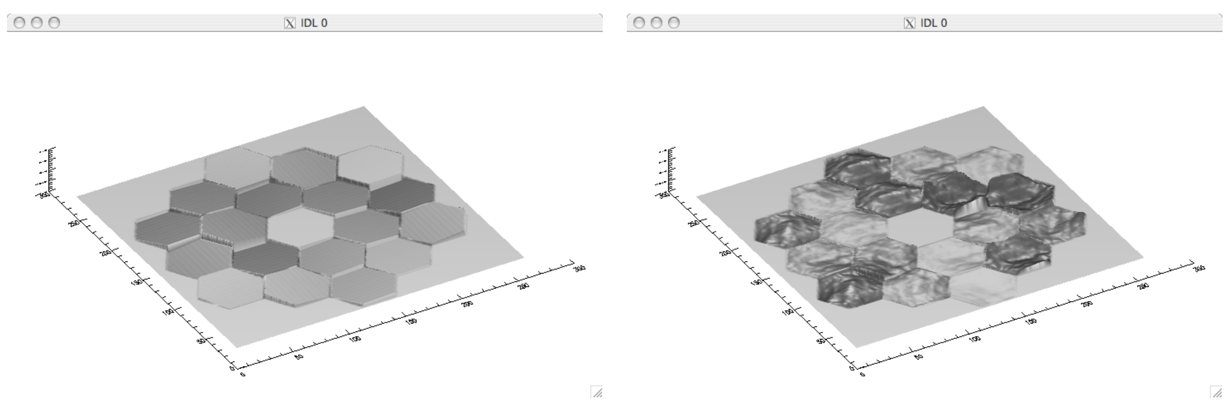

(a) (b)

Figure 3.17-39: A segmented aperture's phase error map for piston, tip, tilt, and flimsy aberrations.

detect motion. Figure 3.17-40(b) demonstrates how the addition of a near-infrared (NIR) band to your data will change motion detection performance. A similar experimental design is evaluated using the spatial target detection algorithm.

The tests reveal how different parameters such as GSD; SNR; spectral band selection; piston, tip, and tilt aberrations; and light weight optic aberrations affect a system's performance.

Project Status:
The project is scheduled to finish in the summer of 2009.

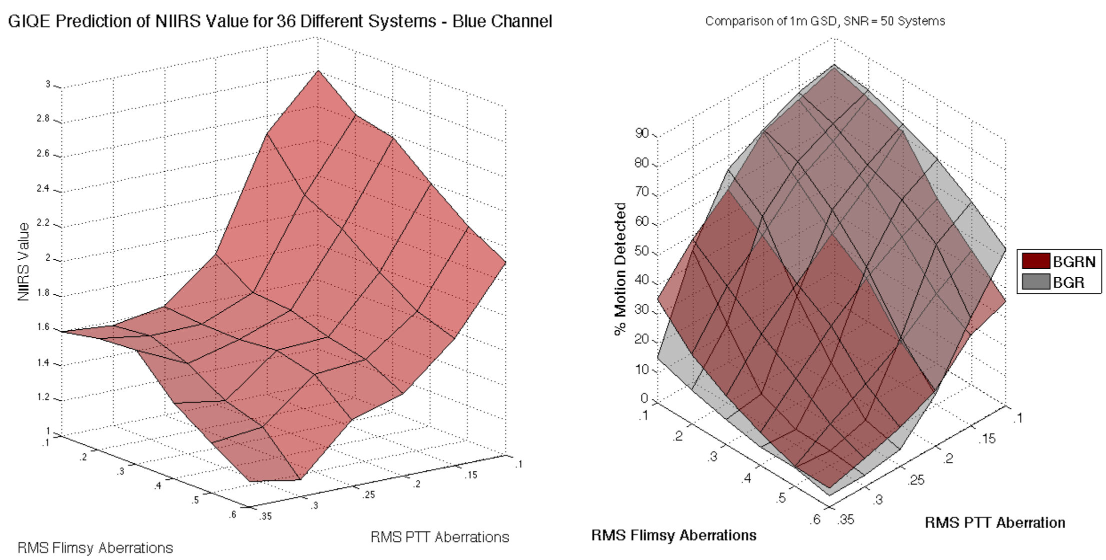

(a) (b)

Figure 3.17-40: Results from the GIQE tests and the motion detection utility tests.

4 RIT Funded Core Research

4.1 DIRSIG Infrastructure

Principal Investigator(s): Mr. Scott Brown
Research Team:Scott Brown, Niek Sanders, Mike Gartley and Adam Goodenough

Project Description:
In addition to the sponsored research projects that address the enhancement of the DIRSIG model, RIT has been slowly increasing the amount of internally funded staff time that is spent working on infra structural DIRSIG development. This ranges from the purchasing and maintenance of the server used to distribute the model to the general maintenance of the software and supporting software development systems. We also internally fund a great deal of the strategic software development that allows us to accomplish research already in-house and compete for new research opportunities. One of the fundamental funding streams for DIRSIG core development has been the DIRSIG Training Courses, which was offered on three (3) different occasions during the last year calendar.

The goal of this project is the continued improvement of the DIRSIG user experience. Specificially, to improve the utility of the tool and integration of the tool with other engineering tools commonly used alongside DIRSIG.

Project Status:
During most of the past year, the development team focused on Release 4.2 The important milestones of that effort was the continued updates to the graphical user interface (GUI) and bringing DIRSIG to the Windows platform. The team has worked very hard to make the GUI an invaluable tool to new and old users. A screen capture of the DIRSIG user interface running under Windows is shown in Figure 4.1-41.

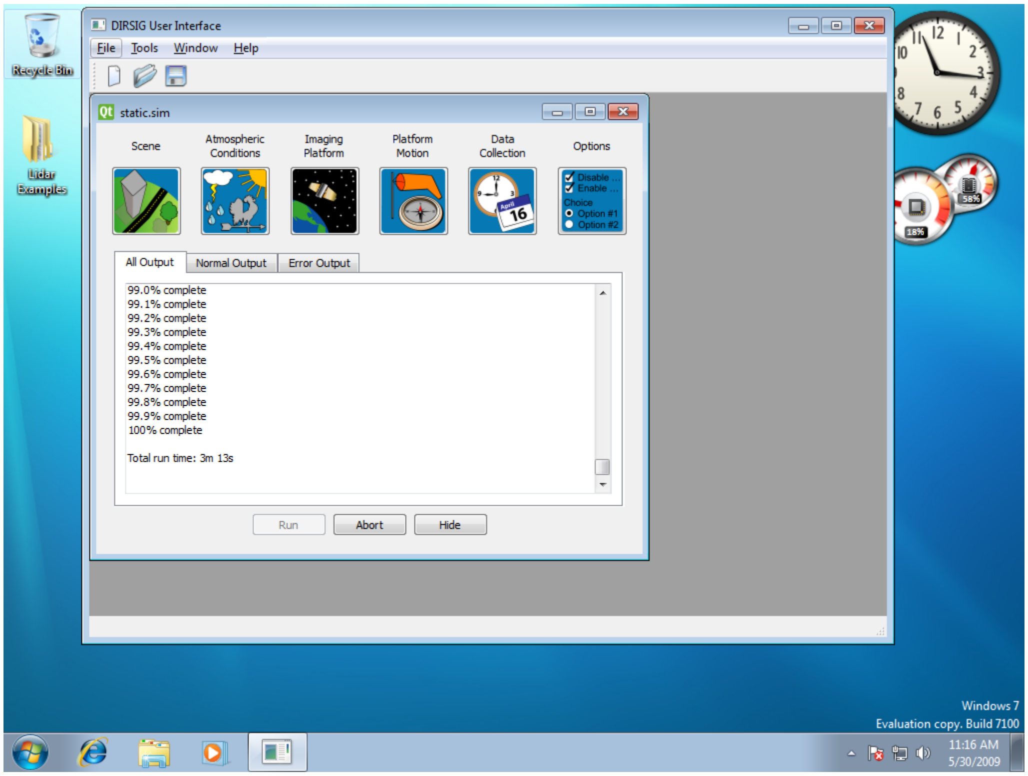

Figure 4.1-41: The main window of the DIRSIG Graphical User Interface (GUI) running under Windows.

The 4.3 release (due for release in Fall 2009) will include some of the most comprehensive improvements to the model over the past few years. These new features will include:

- A new material database editor with interfaces to many of the advanced optical properties available in DIRSIG4.
- New platform jitter models which allow the user to model temporally uncorrelated and correlated jitter.
- The addition of new instrument mounts including the data-driven tabulated mount and the new scripted mount which allows users to write simple programs to define scan patterns.
- Improvements to the channel response model which allow the user to assign linear polarizers (at user-define orientations).
- The ability to use geo-located positions for both scene objects and the platform. This includes a new geo-location truth map that reports the lat/long of each pixel.
- The ability to create and edit a LIDAR instrument from the GUI.
- A set of new platform motion wizards that help the user quickly create specific types of collections. For example, the new ”race track” wizard allows the user to create a platform that circles around a given location.

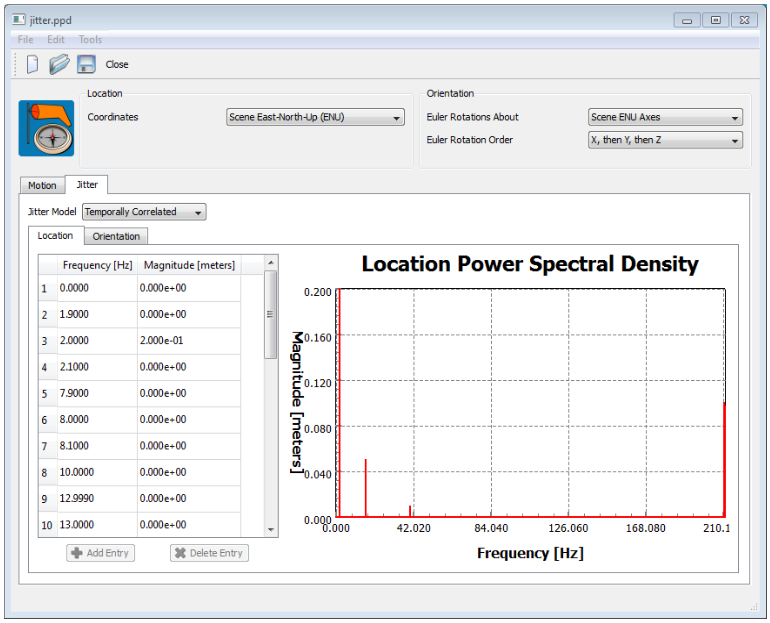

(a) The new temporally correlated jitter model associated with the platform motion.

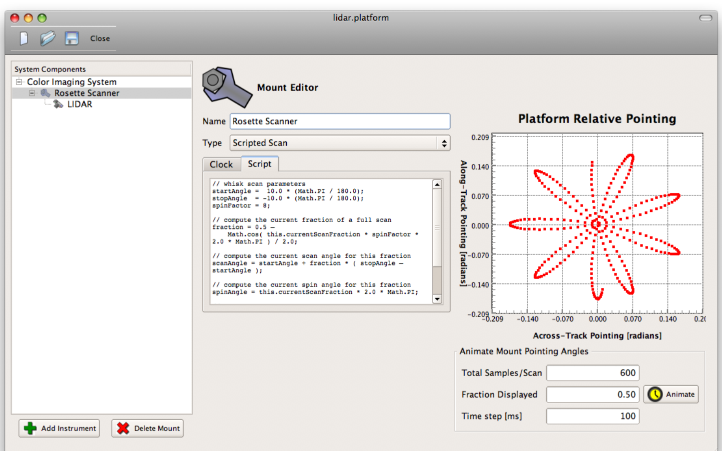

(b) The scriptable instrument mount GUI showing a rosette-style scan pattern described by a user-supplied, 10-line script.

Figure 4.1-42: New DIRSIG User Interfaces for controlling the platform jitter and scan pattern.

During the next year, the development team will continue to provide the user community with improved versions of the DIRSIG model with an increased focus on integration into the modeling workflows used by the user community. This upcoming year will also see the more additions to the new user interface and expanded documentation and training to educate the user community.

4.2 Advanced ANalyst Exploitation Environment (AANEE)

Principal Investigator(s): Dr. John Schott
Research Team: Jake Clements, Karl Walli, & Colin Doody

Project Description:
The tasks of the AANEE project have been split into three portions: development of a three dimensional environment in which to store and interact with the data, advanced 3D registration techniques to relate the multimodal data, and new exploitation tools that utilize the other two as well as feed in new data. Great improvements have been made over the past year as shown in Figure 4.2-43.

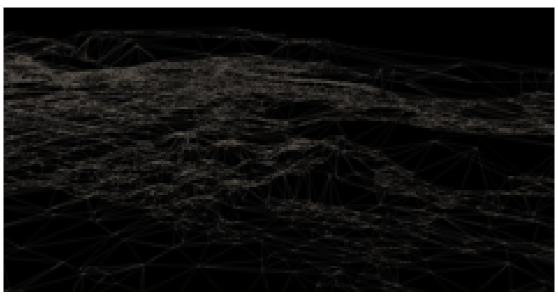

(a) The wire mesh

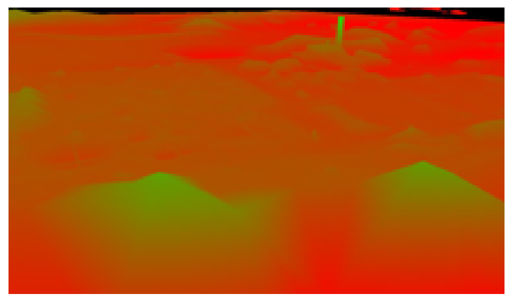

(b) Height information

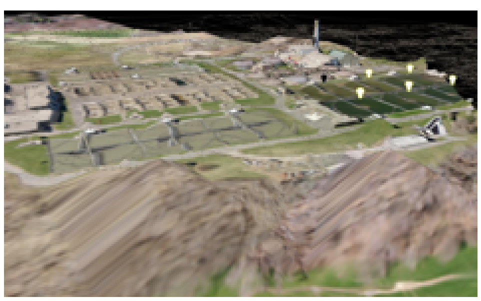

(c) Projection of image onto the mesh

(d) Wastewater flow diagram

Figure 4.2-43: Screen shots of the AANEE software.

The terrain mesh shown in Figure 4.2-43(a) was extracted from a group of five images taken with the WASP sensor. For more information on how that was done see the section on AeroSynth (Sec. 4.3. Figure 4.2-43(b) shows the height information of the wire mesh. In Figure 4.2-43(c) we can see an image projected onto the terrain. Another important feature to note in this figure is the floating light bulbs. These are icons that were inserted by a user in order to mark an observable in the image. Ultimately we plan to be able to scroll through time viewing multiple images and have the various light bulbs flip on and off based upon information extracted from each image. Lastly is the demonstration of the flow diagram evident in Figure 4.2-43(d). This is actually seen in an alternate viewing mode that enables one to turn on and off such process diagrams. Additionally a user can create his/her own sequences. For this particular flow diagram of the wastewater a sequence was created that stopped at each of the pieces of infrastructure. Each piece had a small text box pop up that described its function and, in some cases, the date it was built or installed. Such capabilities are valuable when monitoring a large site over time in order to help refresh the memory of an analyst or to quickly bring a new analyst up to speed on the site of interest. Some steps have also been made toward the exploitation of data using the AANEE tools and by next year we hope to have some results from new exploitation methods. We are working to construct three methods to determine the operational mode of the plant using geometrical, statistical, and template matching approaches. We hope to further differentiate the operational modes into different flavors; *i.e.*, determine the number of pumps that are running and approximate the quality of the effluent flow into Lake Ontario.

Project Status:
This is an ongoing project with completion scheduled in Summer 2010.

4.3 AeroSynth - Airborne Terrain Synthesis

Principal Investigator(s): Dr. John Schott
Research Team: Lt. Col. Karl Walli, Dave Nilosec, Dr. John Schott, Dr. Carl Salvaggio

Project Description:
Automated Airborne Synthetic (AeroSynth) terrain and 3D structure generation is now becoming feasible with calibrated camera remote sensing. This project implements computer vision techniques that have recently become popular to extract structure from motion (SfM) of a calibrated camera with respect to a target. This process builds off of Microsofts popular PhotoSynth technique and applies it to geographic scenes imaged from an airborne platform. Additionally, it will be augmented with new features to increase the fidelity of the 3D structure for realistic scene modeling. This includes the generation of both sparse and dense point clouds useful for synthetic macro/micro-scene reconstruction. This project has been utilizing the CIS departments Wildfire Airborne Sensor Program (WASP) cameras, due to their accessibility and excellent calibration, but, is structured to provide similar capabilities for any calibrated airborne platform.

Although, computer vision has been an active area of research for decades, it has recently experienced a renaissance due to a few significant breakthroughs. This project incorporates the developments in mathematical formalism, robust automated point extraction, and efficient sparse matrix algorithm implementation that have fomented the capability to retrieve 3D structure from multiple aerial images of the same target and apply it to geographical scene modeling. Scenes are reconstructed on both a macro and a micro scale. The macro scene reconstruction implements the scale invariant feature transform to establish initial correspondence, then extracts a scene coordinate estimate using photogrammetric techniques. The estimates along with calibrated camera information are fed through a sparse bundle adjustment to extract refined scene coordinates. The output from this process is the location (X, Y, Z) and orientation (roll, pitch, yaw) of each camera station and the 3D coordinates of thousands of control points in the overlap region of the images (*i.e.*, a sparse point cloud). The micro scale reconstruction derives a denser correspondence of specific targets using the epipolar geometry derived in the macro method. The output from this second stage is a pixel-to-pixel relationship between the images of interest (*i.e.*, a dense point cloud).

The seeds of computer vision were actually planted by photogrammetrists over 40 years ago, through the development of space resectioning and bundle adjustment techniques. But it is only the parallel breakthroughs in the previously mentioned areas of computer vision and computational mathematics that have finally allowed the dream of rudimentary 3D computer vision to be fulfilled in an efficient and robust fashion. Both areas will benefit from the application of these advancements to geographical synthetic scene modeling.

Project Status:
This project is an ongoing element of the DIRS funded AANEE program.

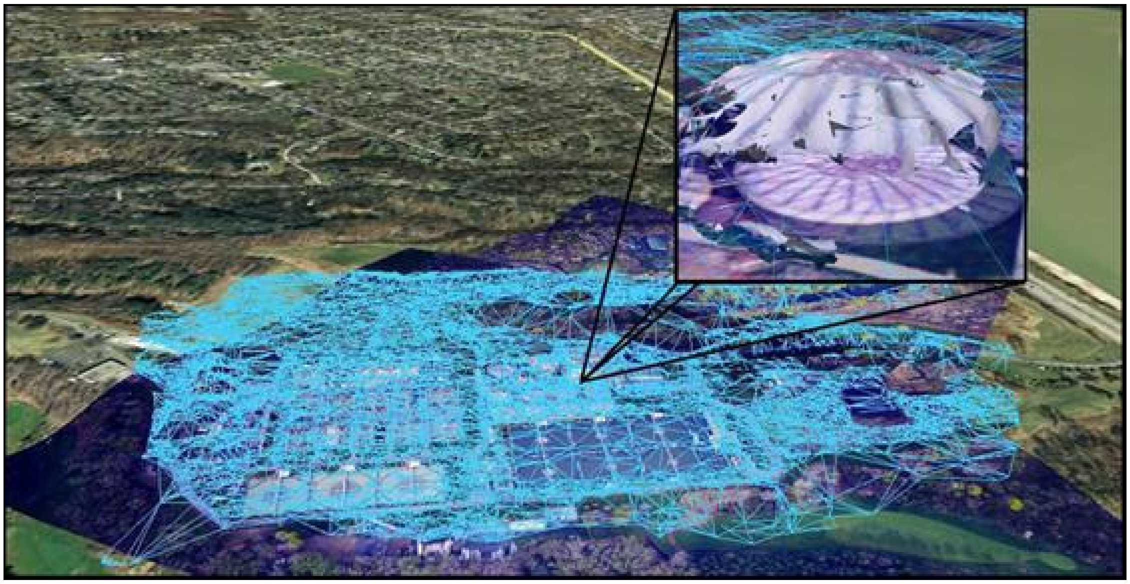

Figure 4.3-44: A sparse point cloud faceted mesh superimposed on a Google Earth background and a highlighted inset of a localized region where a dense point cloud has been developed.

4.4 Validation of Radiative Transfer in Ocean-Water Systems

Principal Investigator(s): Dr. John Schott
Research Team: Jacqueline Speir, Dr. John Schott, Scott Brown, Dr. Adam Goodenough

Project Description:
Sensor reaching radiance in coastal ocean-water environments contains contributions from the air-water interface, in-water objects, and the participating volume itself. In a synthetic image generation model, the expected imagery must account for several interesting phenomenon, including, but not limited to; volumetric scattering, shadows, skyfraction, background reflections, and reflective and transmissive contributions that are a function of capillary and gravity waves (e.g caustics, solar glint, etc.). DIRSIG models the radiative transfer process in this complex environment using a combination of sophisticated raytracing and photon mapping techniques. This research attempts to validate the radiometric modeling process used by DIRSIG when rendering coastal environments with significant contributions from in-water objects.

Project Status:
The validation and verification process has three major phases. The first phase concerns the sequential evaluation of radiometric contributions to sensor reaching radiance. This is accomplished by comparing the DIRSIG modeled results to those predicted analytically, by comparison to other numerical models, and by comparison to observed field and water-tank phenomenology. The second phase addresses image quality concerns that are a function of the type and configuration of DIRSIG radiometry solvers. The primary goal of this phase of the research is to provide the user with a first-order estimate of a radiometry solver's ability to render a given phenomenon, and the expected variance and bias in the generated imagery, given the solver's current configuration. The final phase attempts to demonstrate DIRSIG's ability to model and render complex coastal ocean-water scenes, thereby proving that the phase one validations, when taken in combination, generate realistic and useful imagery.

Recent validation efforts emphasize the radiometric impact of surface related phenomenon. An example

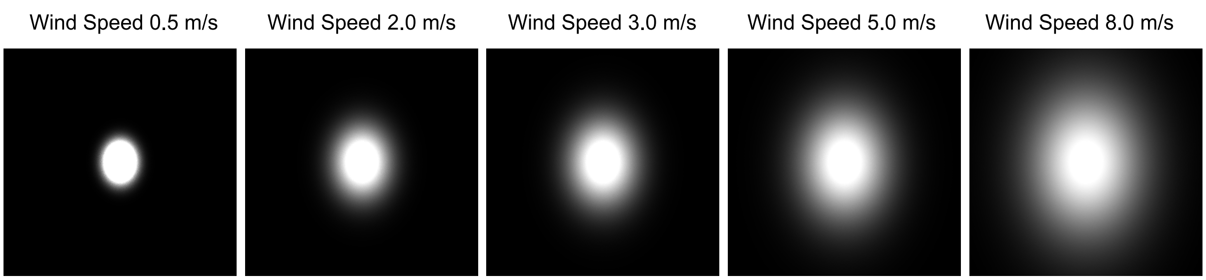

Figure 4.4-45: Solar glint from a wind-roughened air-water interface (images are oriented such that the upwind direction is vertical).

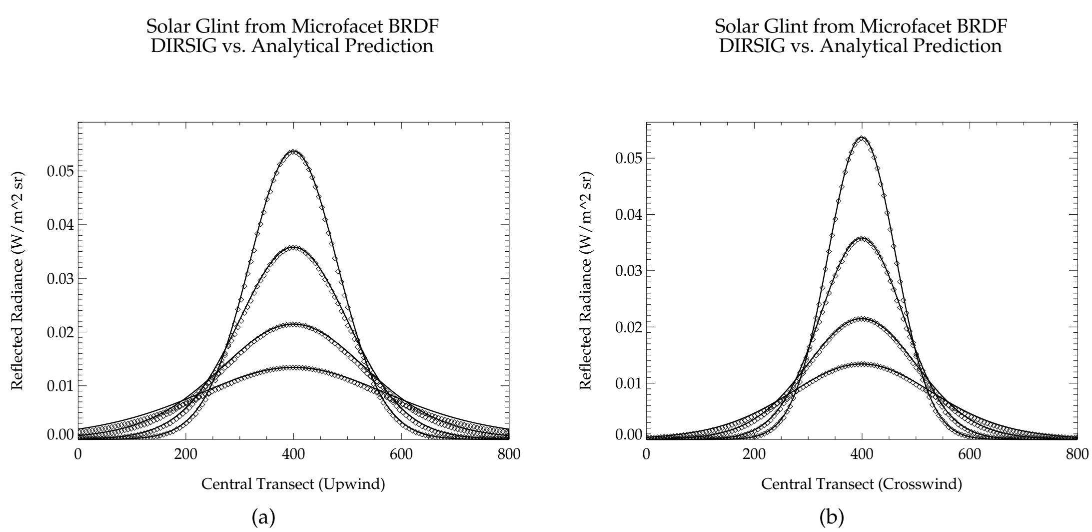

Figure 4.4-46: Agreement between the analytical prediction (solid line) and DIRSIG modeled (diamonds) reflected radiance from the solar disc, shown for 2.0 (most specular), 3.0, 5.0 and 8.0 (most diffuse) $\frac{m}{s}$ wind speeds.

is the bidirectional reflectance distribution function generated by capillary waves on a wind-roughened air-water interface, and the resulting solar glint. Representative imagery showing the reflection of the solar disc for various wind speeds can be seen in figure 4.4-45. Excellent agreement is found when the DIRSIG modeled reflected radiance is compared to that predicted analytically, as shown in figure 4.4-46, for wind speeds of 2.0, 3.0, 5.0 and 8.0 $\frac{m}{s}$.

Another example of an interesting surface-generated effect is the volumetric shadow induced by a floating vessel. In a participating medium, this volumetric void is slowly filled in by the process of multiple scattering. Drawing from numerical simulation results generated by Reinersman & Carder (2004), DIRSIG's ability to model volumetric shadowing and multiple in-scattering was validated. The numerical simulation results are shown in figure 4.4-47. The void in the top central portion of the plot is the floating vessel. The steep vertical downwelling irradiance contours within the participating volume and above the air-water interface (at a depth of 10-meters) show the bounds of the volumetric shadow, and the surface shadow generated by a sun at a solar zenith angle of 30 degrees. The low reflectance of both the vessel and ground plane ensure that the irradiance beneath the vessel is largely a function of in-scattering described by a highly forward-peaked scattering phase function, and a relatively clear water body.

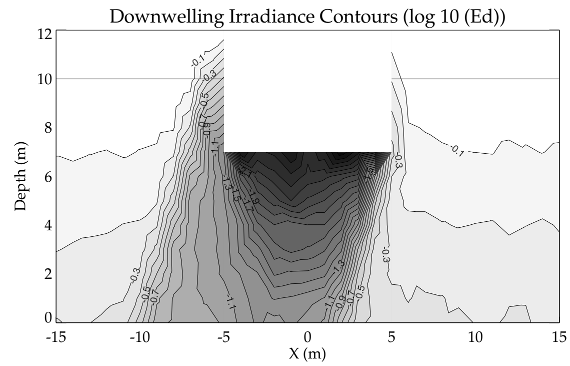

Figure 4.4-47: Downwelling irradiance contours demonstrating surface shadowing, volumetric shadowing, and multiply scattered radiance.

5 The DIRS Annual Research Symposium, June 2 - 3, 2009

The DIRS Annual Research Symposium was another successful event during which the DIRS laboratory presented the accomplishments to invited collaborators, sponsors, and other interested parties over the course of 2 days. Attendance at the symposium by outside visitors was approximately 20 persons across government, industry, and academia. The event was opened by remarks from Dr. Sophia Maggelakis, Dean of the RIT College of Science, and continued with an overview presentation on the "state" of the lab followed by 11 technical talks on Day 1. The second day continued with shorter presentations in three tracks. There were 3 presentations in a track in "Image Analysis"; 4 presentations in the track on "System Analysis", and 4 talks in a track focused on "Modeling". In all, there were 22 technical talks, of which 15 were contributed by graduate students in the DIRS laboratory.

The presentations were recorded and both the videos of the talks and the slides used are available on the DIRS web page at:

http://dirs.cis.rit.edu/special_events/annual_research_symposium/dars2009.

6 Publications During This Period

[1] J. Bishoff, "Target detection using oblique hyperspectral imagery; a domain trade study," MS dissertation, Rochester Institute of Technology, College of Science, Center for Imaging Science, Rochester, New York, United States, 8 2008.

[2] F. Padula, "Historic thermal calibration of the landsat 5 tm through an improved physics based approach," MS dissertation, Rochester Institute of Technology, College of Science, Center for Imaging Science, Rochester, New York, United States, 10 2008.

[3] M. Turk, "A homography-based multiple-camera person-tracking algorithm," MS dissertation, Rochester Institute of Technology, College of Science, Center for Imaging Science, Rochester, New York, United States, 8 2008.

[4] M. Stefanou, *Spectral image utility for target detection applications*. Ph.D. dissertation, Rochester Institute of Technology, College of Science, Center for Imaging Science, Rochester, New York, United States, 8 2008.

[5] S. Klempner, *Statistical modeling of radiometric error propagation in support of hyperspectral imaging inversion and optimized ground sensor network design*. Ph.D. dissertation, Rochester Institute of Technology, College of Science, Center for Imaging Science, Rochester, New York, United States, 10 2008.

[6] B. Daniel, *A System Study of Sparse Aperture Sensors in Remote Sensing Applications with Explicit Phase Retrieval*. Ph.D. dissertation, Rochester Institute of Technology, College of Science, Center for Imaging Science, Rochester, New York, United States, 1 2009.

[7] M. Montanaro, *Radiometric modeling of mechanical draft cooling towers to assist in the extraction of their absolute temperature from remote thermal imagery*. Ph.D. dissertation, Rochester Institute of Technology, College of Science, Center for Imaging Science, Rochester, New York, United States, 5 2009.

[8] Z. Wang, A. Vodacek, and J. L. Coen, "Generation of synthetic infrared remote-sensing scenes of wildland fire," *International Journal of Wildland Fire* **18**, pp. 302–309, 5 2009.

[9] A. Schlamm, D. W. Messinger, and B. Basener, "Geometric estimation of the inherent dimensionality of single and multi-material clusters in hyperspectral imagery," *Journal of Applied Remote Sensing* **3**, 4 2009.

[10] J. C. Makarewicz, T. W. Lewis, I. Bosch, M. R. Noll, N. Herendeen, R. D. Simon, J. Zollweg, and A. Vodacek, "The impact of agricultural best management practices on downstream systems: Soil loss and nutrient chemistry and flux to conesus lake, New York, USA," *Journal of Great Lakes Research* **In press**, 2009.

[11] S. Delalieux, B. Somers, W. Verstraeten, J. van Aardt, W. Keulemans, and P. Coppin, "Hyperspectral indices to diagnose leaf biotic stress of apple plants,considering leaf phenology," *International Journal of Remote Sensing* **30**(8), pp. 1887–1912, 2009.

[12] J. Mandel, L. S. Bennethum, J. D. Beezley, J. L. Coen, C. C. Douglas, M. Kim, and A. Vodacek, "A wildland fire model with data assimilation," *Mathematics and Computers in Simulation* **79**, pp. 584–606, 12 2008.

[13] J. P. Kerekes, K. E. Strackerjan, and C. Salvaggio, "Spectral reectance and emissivity of man-made surfaces contaminated with environmental effects," *Optical Engineering* **47**, pp. 106201/1–106201/10, 10 2008.

[14] M. S. Foster, J. R. Schott, and D. W. Messinger, "Spin-image target detection algorithm applied to low density 3d point clouds," *Journal of Applied Remote Sensing* **2**, 9 2008.

[15] S. R. Lach, J. P. Kerekes, and X. Fan, “Fusion of multiple image types for the creation of radiometrically-accurate synthetic scenes,” *SPIE Journal of Applied Remote Sensing* , 7 2008.

[16] M. S. Stefanou and J. P. Kerekes, “A method for assessing spectral image utility,” *IEEE Transactions on Geoscience and Remote Sensing* , 7 2008.

[17] Y. Li, A. Vodacek, R. L. Kremens, A. J. Garrett, I. Bosch, J. C. Makarewicz, and T. W. Lewis, “Circulation and stream plume modeling in conesus lake.,” *Environmental Modeling and Assessment.* **13**, pp. 175–289, 2008.

[18] J. P. Kerekes, “Receiver operating characteristic curve confidence intervals and regions,” *IEEE Geoscience and Remote Sensing Letters* **5**(2), pp. 251–255, 2008.

[19] J. van Aardt and M. Norris-Rogers, “Spectral age interactions in managed, even-aged eucalyptus plantations: application of discriminant analysis and classification and regression trees approaches to hyperspectral data,” *International Journal of Remote Sensing* **29**(6), pp. 1841–1845, 2008.

[20] J. van Aardt, R. H. Wynne, and J. A. Scrivani, “Lidar-based mapping of forest volume and biomass by taxonomic group using structurally homogenous segments,” *Photogrammetric Engineering and Remote Sensing* **74**(8), pp. 1033–1044, 2008.

[21] W. J. Roberts, J. van Aardt, and F. Ahmed, “Assessment of image fusion procedures using entropy, image quality, and multispectral classification,” *Journal of Applied Remote Sensing* **2**(023522), pp. 1–28, 2008.

[22] B. Majeke, J. A. van Aardt, and M. Cho, “Imaging spectroscopy of foliar biochemistry in forestry environments,” *Southern Forests* **70**(3), pp. 275–285, 2008.

[23] S. Lhermitte, J. Verbesselt, I. Jonckheere, K. Nackaerts, J. A. van Aardt, W. Verstraeten, and P. Coppin, “Hierarchical image segmentation based on similarity of ndvi time series,” *Remote Sensing of Environment* **112**, pp. 506–521, 2008.

[24] P. Kempeneers, P. Zarco-Tejada, P. North, S. D. Backer, S. Delalieux, G. Sepulcre-Canto, F. Morales, J. van Aardt, R. Sagardoy, P. Coppin, and P. Scheunders, “Model inversion for chlorophyll estimation in open canopies from hyperspectral imagery,” *International Journal of Remote Sensing* **29**(17-18), pp. 5093–5111, 2008.

[25] M. Gebreslasie, F. Ahmed, and J. van Aardt, “Estimating plot-level forest structural attributes using high spectral resolution aster satellite data in even-aged eucalyptus plantations in southern kwazulu-natal, south africa,” *Southern Forests* **70**(3), pp. 227–236, 2008.

[26] M. Montanaro, C. Salvaggio, S. D. Brown, D. W. Messinger, A. J. Garrett, and J. S. Bollinger, “Radiometric modeling of mechanical draft cooling towers to assist in the extraction of their absolute temperature from remote thermal imagery,” in *Proceedings of the SPIE, SPIE Defense and Security, Thermosense XXXI, Infrared Sensors and Systems*, **7299**, SPIE, (Orlando, Florida, United States), 4 2009.

[27] M. V. Arsenovic, C. Salvaggio, A. J. Garrett, B. D. Bartlett, J. W. Faulring, R. L. Kremens, and P. S. Salvaggio, “Use of remote sensing data to enhance the performance of a hydrodynamic simulation of a partially frozen power plant cooling lake,” in *Proceedings of the SPIE, SPIE Defense and Security, Thermosense XXXI, Infrared Sensors and Systems*, **7299**, SPIE, (Orlando, Florida, United States), 4 2009.

[28] S. Higbee, D. W. Messinger, Y. Tra, J. Voelkel, and L. Chilton, “A bayesian approach to identi?cation of gaseous efuents in passive lwir imagery,” in *Proceedings of SPIE, Defense and Security Symposium, Algorithms and Technologies for Multispectral, Hyperspectral, and Ultraspectral Imagery XV*, **7334**, SPIE, (Orlando, Florida, United States), 4 2009.

[29] T. Doster, D. Ross, D. W. Messinger, and B. Basener, "Anomaly clustering in hyperspectral images," in *Proceedings of SPIE, Defense and Security Symposium, Algorithms and Technologies for Multispectral, Hyperspectral, and Ultraspectral Imagery XV*, **7334**, SPIE, (Orlando, Florida, United States), 4 2009.

[30] B. Basener and D. W. Messinger, "Enhanced detection and visualization of anomalies in spectral imagery," in *Proceedings of SPIE, Defense and Security Symposium, Algorithms and Technologies for Multispectral, Hyperspectral, and Ultraspectral Imagery XV*, **7334**, SPIE, (Orlando, Florida, United States), April 2009.

[31] M. Gebreslasie, F. Ahmed, and J. A. van Aardt, "Extracting forest structural attributes in south africa using image texture analysis and artificial neural networks from ikonos imagery," in *, Proceedings of the 33rd International Symposium on Remote Sensing of Environment, May 4-8, 2009*, RSE, (Stresa, Piemonte, Italy), 2009.

[32] A. Schlamm, D. W. Messinger, and B. Basener, "Effect of manmade pixels on the inherent dimension of natural material distributions," in *Proceedings of SPIE, Defense and Security Symposium, Algorithms and Technologies for Multispectral, Hyperspectral, and Ultraspectral Imagery XV*, **7334**, SPIE, (Orlando, Florida, United States), 2009.

[33] J. Bishoff, D. W. Messinger, and E. J. Ientilucci, "Oblique hyperspectral target detection," in *Proceedings of SPIE, SPIE Optic and Photonics, Imaging Spectrometry XIII*, **7086**, SPIE, (San Diego, California, United States), 8 2008.

[34] M. Montanaro, C. Salvaggio, D. W. Messinger, S. D. Brown, and A. J. Garrett, "Apparent temperature dependence on localized atmospheric water vapor," in *Proceedings of the SPIE, SPIE Defense and Security, Sensor Data Exploitation and Target Recognition, Algorithms and Technologies for Multispectral, Hyperspectral, and Ultraspectral Imagery XIV*, **6966**, pp. 1505–1516, SPIE, (Orlando, Florida, United States of America), 4 2008.

[35] D. Gillis, J. Bowles, E. J. Ientilucci, and D. W. Messinger, "A generalized linear mixing model for hyperspectral imagery," in *Proceedings of SPIE, Defense and Security Symposium, Algorithms and Technologies for Multispectral, Hyperspectral, and Ultraspectral Imagery XIV*, **6966**, SPIE, (Orlando, Florida, United States), 4 2008.

[36] D. W. Messinger, C. Salvaggio, and N. M. Sinisgalli, *Spectral Sensing Research for Water Monitoring Applications and Frontier Science and Frontier Science, and Technology for Chemical, Biological and Radiological Defense*, vol. 48 of *Selected Topics in Electronics and Systems*, ch. Detection of gaseous effluents from airborne LWIR hyperspectral imagery using physics-based signatures. World Scientific Publishing Company, Hackensack, New Jersey, United States, 1st ed., 12 2008.

[37] J. D. Beezley, S. Chakraborty, J. L. Coen, C. C. Douglas, J. A. Mandel, A. Vodacek, and Z. Wang, *Computational Science ICCS 2008*, vol. 5103 of *Lecture Notes in Computer Science*, ch. Real-Time Data Driven Wildland Fire Modeling. Springer, Berlin, Berlin, Germany, 2008.

[38] S. E. Paul, D. R. Nilosek, D. W. Messinger, and C. Salvaggio, "Derivation of radiometric temperature for sub-pixel targets from thermal infrared imagery using three-dimensional physical modeling techniques," in *University and Industry Technical Interchange Review Meeting, UITI 2008*, Department of Energy NA-22, (Park City, Utah, United States), 12 2008.

[39] R. V. Raqueno and C. Salvaggio, "The practicals of grid computing with envi/idl: Case studies in high throughput computing (htc) using condor and envi/idl for physics-based remote sensing algorithms and applications," in *ENVI User Symposium (ENVIUS 2008)*, ITTVIS, (Chantilly, Virginia, United States of America), 5 2008.